Turkish Journal of Earth Sciences

Volume 33 | Number 2 Article 3

1-29-2024

Genesis of efficient reservoirs in mixed sedimentary setting: a case study of Benxi Formation in the Gaoqiao area, Ordos Basin

SHU LIU
2015914@cqust.edu.cn

JINBU LI
ljb2_cq@petrochina.com.cn

FENGBO JIN
jinfb_cq@petrochina.com.cn

HAIFENG LIU
liuhaif_cq@petrochina.com.cn

MENG WANG
wangmeng_cqust@126.com

See next page for additional authors

Recommended Citation

LIU, SHU; LI, JINBU; JIN, FENGBO; LIU, HAIFENG; WANG, MENG; CHENG, YULIN; CHENG, YULIN; ZHONG, XIAOHONG; and LU, HAO (2024) "Genesis of efficient reservoirs in mixed sedimentary setting: a case study of Benxi Formation in the Gaoqiao area, Ordos Basin," *Turkish Journal of Earth Sciences*: Vol. 33: No. 2, Article 3. https://doi.org/10.55730/1300-0985.1903
Available at: https://journals.tubitak.gov.tr/earth/vol33/iss2/3

Genesis of efficient reservoirs in mixed sedimentary setting: a case study of Benxi Formation in the Gaoqiao area, Ordos Basin

Authors

SHU LIU, JINBU LI, FENGBO JIN, HAIFENG LIU, MENG WANG, YULIN CHENG, YULIN CHENG, XIAOHONG ZHONG, and HAO LU

Turkish Journal of Earth Sciences

http://journals.tubitak.gov.tr/earth/

Research Article

Turkish J Earth Sci
(2024) 33: 118-145

doi:10.55730/1300-0985.1903

Genesis of efficient reservoirs in mixed sedimentary setting: a case study of Benxi Formation in the Gaoqiao area, Ordos Basin

Shu LIU[1,2,3,*], Jinbu LI[4], Fengbo JIN[4], Haifeng LIU[4], Meng WANG[1,2,3,4,5] Yulin CHENG[6], Xiaohong ZHONG[5], Hao LU[2]

[1]School of Petroleum Engineering, Chongqing University of Science and Technology, Chongqing, China
[2] Chongqing Zhiyou Shuyan Technology Co., Ltd, Chongqing, China
[3]Natural Gas Geology Key Laboratory of Sichuan Province, Southwest Petroleum University, Chengdu, Sichuan Province, China
[4]Research Institute of Exploration and Development, PetroChina Changqing Oilfield Company, Xi'an, China
[5]National University Science Park, Southwest Petroleum University, Chengdu, Sichuan Province, China
[6]College of Petroleum Engineering, China University of Petroleum, Beijing, China

Received: 11.04.2023 • **Accepted/Published Online:** 17.12.2023 • **Final Version:** 29.01.2024

Abstract: The Benxi-Taiyuan Formation in the southern region of the Ordos Basin represents a typical mixed sedimentary system, which has witnessed recent breakthroughs in the exploration of tight sandstone gas within the Benxi Formation. However, the development patterns of reservoirs in this mixed sedimentary area remain unclear, influenced by the sedimentary model and the distribution scale of sedimentary sandstone bodies. This study investigates the paleogeomorphology, sedimentary model, sandstone body type, petrological characteristics, and pore structure of the Benxi Formation. Field profiles, drilling core observations, microscopic section analysis, scanning electron microscopy (SEM), high-pressure mercury injection (HPMI), and physical property analysis are employed. The findings indicate that the paleogeomorphology before the deposition of the Benxi Formation exhibits a west-to-east high-to-low trend, with a steeper gradient in the north and a gentler gradient in the south. This paleogeomorphology influences paleocurrent direction and the distribution of sandstone bodies. The sedimentary system, consisting of clastic tidal flats, mixed tidal flats, and mixed lagoons, develops from west to east on a plane, with the mixed lagoon being more prominent in the northeast of the study area. The sedimentary model determines the initial composition and structure of the reservoir, as well as subsequent diagenesis processes. Diagenetic reconstruction plays a crucial role in assessing the development degree of reservoir. Compaction and cementation result in the densification of the Benxi Formation sandstone. Dissolution and preservation of primary pores are critical for high-quality reservoir development. Among the various depositional models, the sand flat facies in the clastic tidal flat area of the Ben 2 Member and the tidal channel facies in the mixed tidal flat areas of the Ben 1 and Ben 2 members exhibit a high degree of pore development within the sandstone body, making them favorable locations for high-quality reservoir development. In summary, this study highlights the importance of paleogeomorphology, sedimentary models, and diagenetic reconstruction in understanding the controlling factors for efficient reservoir development in the mixed sedimentary system of the Benxi-Taiyuan Formation. Knowledge of these factors aids in the exploration of high-quality reservoirs within concealed and dispersed sandstone formations in the Ordos Basin.

Key words: Mixed sedimentary type, efficient reservoirs, sedimentary facies, diagenesis, Benxi Formation, Ordos Basin

1.Introduction

The Ordos Basin, located in China, is a significant natural gas production area, housing a substantial proportion of tight gas reserves. Over the past few decades, several large-scale tight sandstone gas fields have been discovered in the basin (Wei and Wang, 2004; Wang, 2014; Dong et al., 2020; Qiao et al., 2020; Ran and Zhou, 2020; Zheng et al., 2020). The tight gas reservoirs within the Ordos Basin are characterized by multiple gas-bearing layers and various reservoir types. Initial exploration efforts primarily focused on the Lower Permian Shanxi Formation and the 8th Member of the Middle Permian Shihezi Formation in the northern part of the basin (Huang et al., 2009; Fu et al., 2013; Jiu et al., 2021). However, progress in the exploration and development of other strata in the southern part of the basin was relatively slow (Guo et al., 2009; Fu et al., 2017). In recent years, attention has turned to the exploration of tight sandstone reservoirs within the Carboniferous Benxi Formation in the southern part of the Ordos Basin, which has shown promising results. Numerous high-yield industrial gas wells have been drilled, leading to a growing interest in this area.

* Correspondence: 2015914@cqust.edu.cn

The Paleozoic era in the Ordos Basin has witnessed a significant evolution of sedimentary environments, transitioning from marine facies to marine-continental transitional facies, and finally to continental facies. Within the Upper Paleozoic, the Carboniferous to Permian strata are characterized by typical marine-continental transitional facies (Cui and Radwan, 2022). Initially, exploration efforts primarily focused on sandstone reservoirs found in extensive areas with continuously distributed sandstone bodies. These bodies were formed by a combination of meandering river delta systems and braided river delta systems, predominantly influenced by Permian fluvial action (Li et al., 2010; Li et al., 2016; Liang et al., 2018). However, recent studies have increasingly examined the sedimentary facies of the Carboniferous Benxi Formation. The current understanding suggests that the sedimentary facies of the Carboniferous Benxi Formation in the Ordos Basin include barrier island-lagoon coastal deposits, a tide-dominated bay-delta environment in the presence of an open epicontinental sea, and a composite sedimentary environment consisting of tidal barriers and deltas (Liu et al., 2018; Liu et al., 2021). However, deciphering the distribution of these sedimentary facies poses challenges, primarily due to several factors such as the relatively small scale of sandstone bodies, limited continuity, and strong heterogeneity. Consequently, this lack of clarity impedes the ability to provide sufficient support for effective exploration and development initiatives.

Numerous exploration practices have indicated that the Carboniferous Benxi Formation in the study area commonly exhibits a sedimentary occurrence characterized by the coexistence of terrigenous clastics and carbonate rocks (Liu et al., 2018). Clarifying the genetic mechanism of sandstone within the context of mixed deposition is the primary challenge when analyzing the distribution patterns of sandstone bodies, the characteristics of effective reservoirs, and the controlling factors for efficient reservoir development. (Hodgkinson et al., 2008; Bezzi et al., 2019; Anees A et al., 2022).

The primary objective of this study is to investigate sedimentary facies and the genesis mechanism of efficient reservoirs within the context of mixed deposition, with a focus on paleogeomorphic restoration. Paleogeomorphology plays a dual role in controlling the development and evolution of sedimentary systems. It not only influences the local hydrodynamic conditions but also governs the distribution patterns of sediment dispersion systems in specific areas. Particularly in mixed sedimentary settings, multiple factors exert control over the development of high-quality reservoirs. Through sedimentary research based on paleogeomorphology, the distribution and extent of dominant sand bodies can be unveiled, which is crucial for effective reservoir prediction and improving exploration success rates. Compared to single clastic rock deposits, high-quality reservoirs in mixed sedimentary backgrounds are subject to a more complex array of controlling factors. Therefore, studying the reservoir pore structure, diagenesis, and other aspects in different regions and sedimentary facies types using the constructed sedimentary model is not only significant for deciphering the genetic laws of efficient gas reservoirs in the study area, but can also serve as a valuable reference for the investigation of similar gas reservoirs.

2. Geological background

The Ordos Basin is situated on the western margin of the North China Craton and is characterized by the presence of six distinct tectonic units: the Yimeng uplift, the Weibei uplift, the western Shanxi flexural fold belt, the northern Shaanxi slope, the Tianhuan depression, and the western margin thrust belt (Liu et al., 2016). The Gaoqiao area is positioned south of the Yishan slope and exhibits relatively minor basement fluctuations. The area is characterized by a relatively flat topography with gentle rises and falls, presenting a nose-shaped structure in the west and a west-inclined slope in the east. The strata are gently inclined, showing rare occurrences of folds (Figure 1a).

Following uplift and denudation in the Early Paleozoic era, the North China Craton underwent near-peneplanation by the early Late Carboniferous period before experiencing a subsequent overall subsidence that facilitated sediment deposition. During the Late Paleozoic era, the Ordos Basin was divided into two distinct sea areas, east and west, by the central paleo-uplift. The eastern region witnessed the intrusion of seawater from the North China Sea, expanding westward (Figure 1b). The westward sedimentation resulted in the formation of a wedge-shaped deposit, characterized by thickness increasing towards the east and thinning towards the west. This sedimentary wedge comprises a mixed deposit comprising interbedded terrigenous clastics, coal seams, and carbonate rocks (Liu et al., 2014; Liu et al., 2021). The factors influencing this mixed sedimentary series are intricate (Li et al., 2014). During the Late Carboniferous period, the basin experienced gradual subsidence with a diminished supply of terrigenous clastic materials, resulting in slow compensational sedimentation. Additionally, an epicontinental sea developed in the eastern region of the central paleo-uplift, featuring a gentle slope and shallow waters. This rapid and abrupt transgression, coupled with frequent sea level fluctuations, facilitated the extensive lateral migration of sedimentary facies, resulting in mixed sedimentation between the adjacent terrigenous clastics and carbonate sedimentary systems (Liu et al., 2018; Liu et al., 2021).

The Gaoqiao area is situated in the eastern region of the central paleo-uplift within the Ordos Basin. Within this area, the Late Carboniferous Benxi Formation overlays the Ordovician paleo-weathering crust, with the top boundary marked by the underlying limestone of the Taiyuan Formation. The thickness of the Benxi Formation ranges from approximately 10 m to 75 m, exhibiting an east-west overlapping distribution pattern (Liu et al., 2018). The lower part of the Benxi Formation consists of a ferriferous clay layer, while the upper portion is predominantly comprised of dark gray or grayish-black mud shale and light gray or grayish-white quartz sandstone. Intercalated within these strata are layers of limestone and coal seams, with the limestone mainly concentrated in the northeast area of the study region (Shen et al., 2009). Moreover, the coal seam exhibits a consistent and stable distribution throughout the entire area (Figure 1c).

The sedimentation phase of the Benxi Formation in the study area was characterized by a dual-source system flowing in a north-south direction (Jia et al., 2019; Li et al., 2019). The two primary sources were the Yinshan-Alashan ancient land located to the north of the basin, and the Qilian-North Qinling ancient land situated to the south, with additional contributions coming from the Liupanshan old land in the southwest. The sedimentary processes in the study area were predominantly controlled by the southwest provenance originating from the western region of the North Qilian (Zhang et al., 2021).

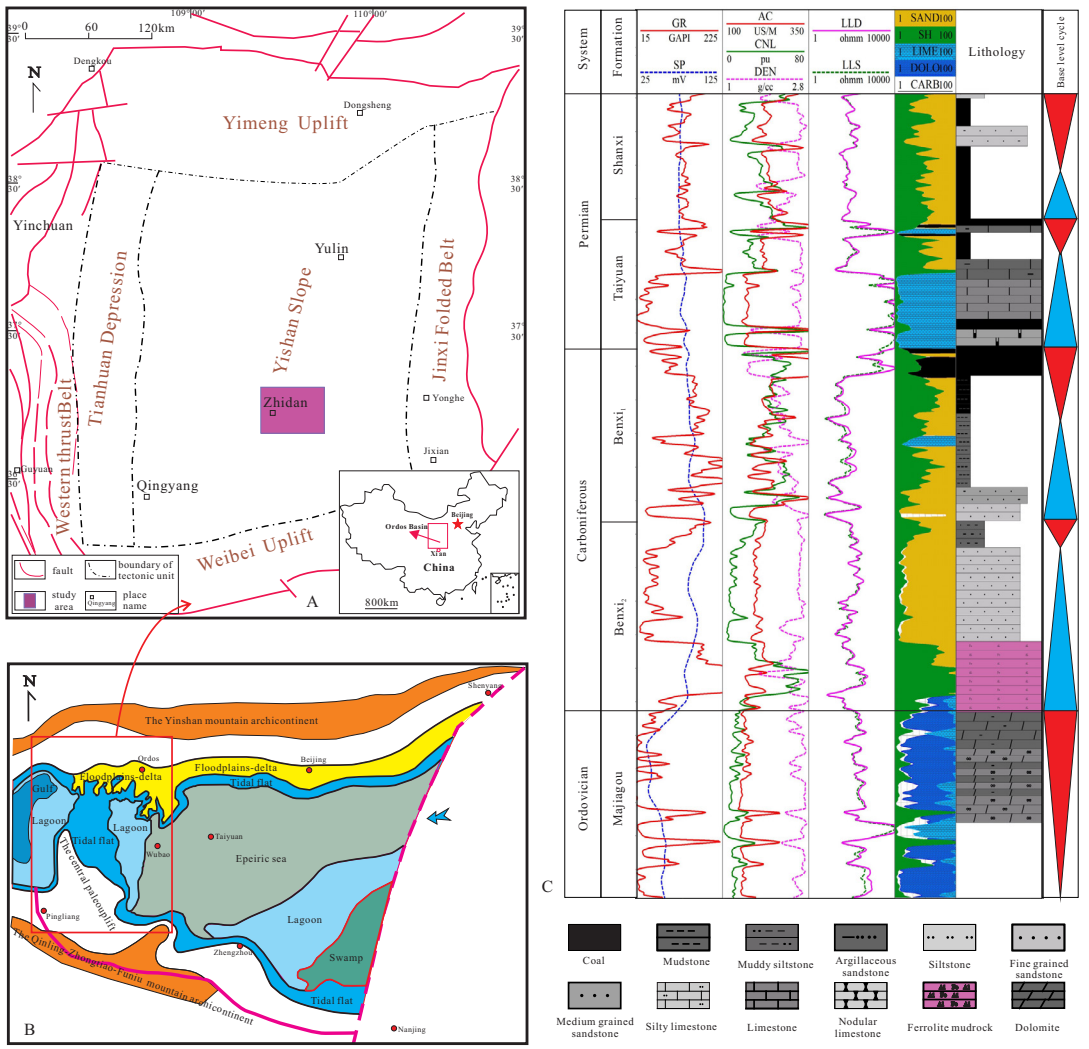

Figure 1. a. Location of the study area and tectonic units of the Ordos Basin, b. tectonic-sedimentary pattern in north China of late Carboniferous (He et al., 2022), c. generalized stratigraphic column of Benxi formation in the Gaoqiao area. (GR: gamma ray; SP: spontaneous potential; AC : acoustic; CNL: neutron; DEN: density; LLD: deep investigate induction log; LLS: shallow investigate induction log; SAND: sand content; SH: shale content ; LIME: limestone content; DOLO: dolomite content; CARB: carbon content.)

3. Materials and methods

To conduct an in-depth investigation into the sedimentation and diagenesis characteristics of the reservoir, this study collected logging response data from over 300 wells and core data from 12 coring wells. Through an analysis of lithology, sedimentary structures, and logging data, the sedimentary facies were determined, and a sedimentary facies distribution map was generated. Furthermore, by clarifying the key stratigraphic marker interface features, the paleogeomorphic conditions prior to the deposition of the Benxi Formation were reconstructed utilizing the impression method.

A total of 210 polished thin sections were prepared using vacuum impregnation with red epoxy resin to analyze the composition and textural characteristics. Some thin sections were stained with Alizarin Reds and K-ferricyanide for the identification of carbonate cement. Thin sections were examined under an LV100PO polarized optical microscope (Nikon).

To examine the microscopic pore structure and cement minerals of the samples, 30 selected samples underwent scanning electron microscope (SEM) tests using an FEI Quanta 200 for analysis. The pores in the SEM images were extracted and measured using PerGeos software from the FEI.

Porosity and permeability tests were conducted on 120 core plungers with a diameter of 1 inch using a CMS-300 physical property tester, under a net confining pressure of 3.5 MPa. Nitrogen gas was employed to determine permeability, and all these samples were matched with thin sections. Based on the results of the porosity and permeability tests, high-pressure mercury injection (HPMI) tests were performed on 40 samples of three distinct pore-developed sandstones using the Quanta Chrome Poremaster-60 mercury injection apparatus, enabling the construction of capillary pressure curves, as well as the determination of threshold pressure and maximum mercury saturation.

To compare the physical property distribution of single sandstone bodies in the Ben1 and Ben2 formations, whisker box diagrams were utilized to compare the physical properties of different sedimentary facies and sandstone body structures.

4. Results

4.1 Paleogeomorphic characteristics before Benxi Formation sedimentation

In the analysis of sedimentary facies, paleogeomorphology holds key importance in determining the distribution of later sediments, particularly in the context of the complex mixed sedimentary background of the Benxi Formation. The characteristics of sandstone bodies and lithology exhibit significant variation across different regions (Yan et al., 2016). Therefore, the restoration of paleogeomorphology in the sedimentary area plays a crucial role in defining the distribution characteristics of high-quality reservoirs.

There are several methods available for the recovery of paleogeomorphology, including the paleogeological method, sequence stratigraphy recovery method, residual thickness method, and impression method (Zhao et al., 2003). Among these, the impression method holds particular significance due to its consideration of the influence of presedimentary structures and its extensive application in various cases. This method establishes an isochronal surface, considering the end of denudation of the landform to be recovered and the beginning of deposition of the overlying strata. It utilizes the mirror image relationship between the overlying strata and the residual paleogeomorphology to semiquantitatively restore the shape of the paleogeomorphology based on the thickness of the overlying strata. In this study, the thickness of the Benxi Formation below the limestone marker bed, located at the base of the Taiyuan Formation, which overlies the Benxi Formation, is divided. The accumulated thickness from the marker bed to the bottom of the Benxi Formation is then employed to mirror the paleogeomorphology.

The Ben 2 member exhibits a thickness ranging from 0.3 m to 55 m, with an average thickness of 15.5 m. The marker bed in this member consists of limestone. The predominant lithology is dark gray mudstone with grayish white fine siltstone, while a conglomerate layer of approximately 2 m thick is developed at the base. Logging data indicates low gamma ray (GR) values and high resistance for this member. As for the Ben 1 member, it has a thickness ranging from 4.8 m to 56 m, with an average thickness of 26.5 m. The boundary between the Ben 1 and Ben 2 members is marked by the presence of sandstone at the bottom of the Ben 1 member. Separating the Benxi Formation from the Taiyuan Formation is a coal seam. At the base of the Ben 1 member, there is a consistent occurrence of grayish white medium-coarse quartz sandstone with a thickness ranging from 5 m to 10 m, which is distributed uniformly across the entire area. The Ben 1 member serves as the primary source rock and gas-producing interval within the Benxi Formation, making it the focus of this study.

The paleogeomorphology of the study area before the deposition of the Benxi Formation exhibits a general pattern of high elevation in the west and low elevation in the east, with a steep slope in the north and a gentle slope in the south. This configuration forms a combination of highlands, slopes, grooves, and a lake basin extending from the southwest to the northeast. The Ben 1 and Ben 2 members overlap from east to west in

this region. The formation of this landform was largely influenced by the regional tectonic framework of the Late Carboniferous craton. Notably, this framework gradually shifted from a "south uplift dipping north" pattern to a "north uplift dipping south" pattern during the Middle Carboniferous (Liu et al., 2018; Liu et al., 2021). Based on the paleogeomorphic characteristics, it can be reasonably inferred that the prevailing paleocurrent direction before the deposition of the Benxi Formation was primarily oriented from the west and southwest towards the east and northeast. This inference aligns with the distribution pattern observed in fluid potential analysis (Figure 2).

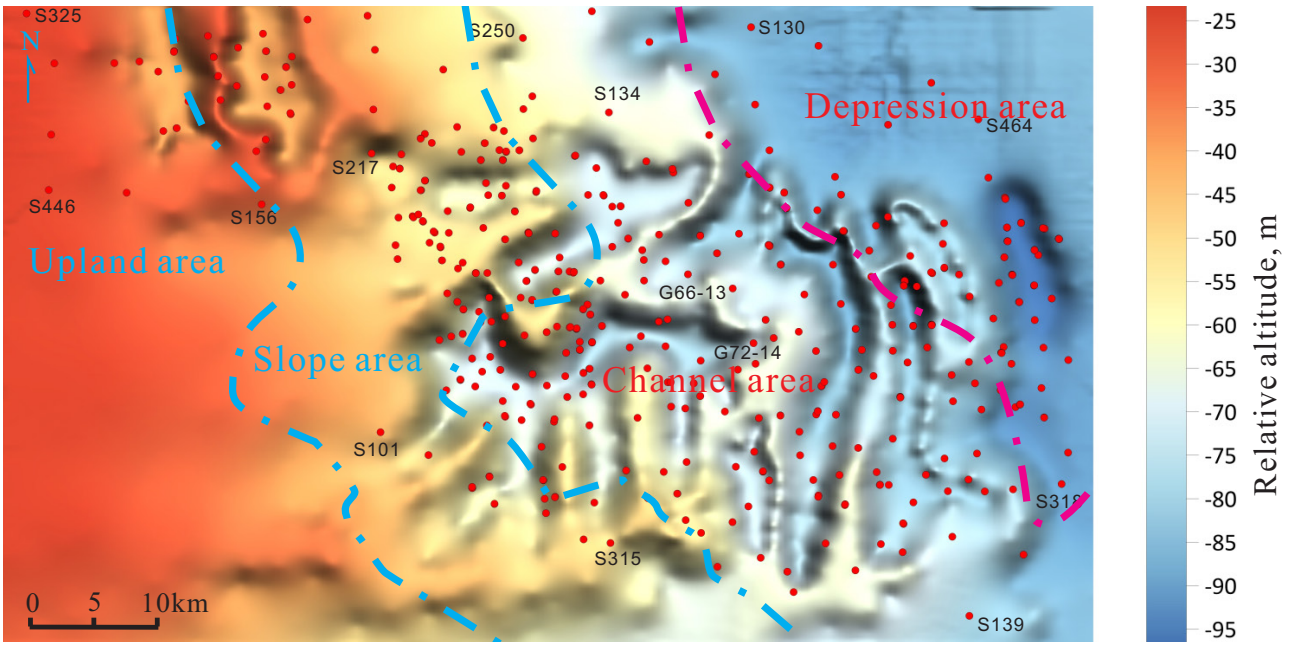

Figure 2. The paleogeomorphology of before Benxi Formation sedimentation, generally, the study area developed upland, slope, channel, depression areas from west to east.

4.2 Sedimentary facies type and distribution

4.2.1 *Sedimentary microfacies division*

The core observation reveals that the rock types of the Benxi Formation consist predominantly of clastic rock and carbonate rock. The clastic rocks mainly include pebbly sandstone, sandstone, siltstone, mudstone and their transitional forms, and the coal streak or coal seam is also developed at the uppermost layer. Conglomerate and sandstone are mainly grayish white, gray, and dark gray (Figure 3). Sandstone comprises mainly medium-fine grained sandstone and limy fine sandstone, while mudstone and carbonaceous mudstone appear predominantly black and grayish black, reflecting the reducing environmental characteristics during sediment formation. Carbonate rocks are mainly limestone and marl.

Core observations indicate that the lithology of the Benxi Formation mainly consists of clastic and carbonate rocks. The clastic rock types encompass pebbly sandstone, sandstone, siltstone, mudstone, along with transitional variations, and are accompanied by the occurrence of coal streaks or coal seams in the upper portion. The predominant colors observed in conglomerates and sandstones are grayish white, gray, and dark gray (Figure 3). The sandstone primarily exhibits a medium-fine grain size and may contain limy fine sandstone. Mudstones and carbonaceous mudstones tend to appear black or grayish black, indicating a reducing sedimentary environment. Carbonate rocks within the formation consists primarily of limestone and marl.

Interestingly, the grain size within the Benxi Formation shows a fining-upward trend, with normal grading observed from the bottom to the top. The sandstone bodies exhibit a thickness ranging from 1 m to 16 m, characterized by the presence of conglomerates and gravel-bearing sandstones at their base (Figures 3a–3c). Irregular scouring surfaces are visible (Figures 3d and 3e), and upwardly, the sandstone reveals a prominent development of tidal bedding structures, such as wedge-shaped cross bedding, tabular cross bedding, and ripple cross bedding (Figures 3f–3i). Vein bedding and lenticular bedding are observed in the upper layers of marlstone, grayish black mudstone, and gray mudstone (Figure 3j). Occasional

occurrences of pyrite and siderite nodules can be seen in the mudstone (Figure 3k), particularly in close proximity to the coal seam at the top (Figure 3l).

The typical bedding characteristics in the sand layer are as follows:

(1) Massive bedding: Massive bedding appears relatively homogeneous in both structure and composition, lacking distinct layering or laminae structures. The absence of obvious stratification can be attributed to rapid sediment gravity flow and the uniform deposition of well-sorted clastic materials, indicating relatively stable hydrodynamic conditions (Figures 3a–3c).

(2) Scour surface: A scour surface refers to an uneven deposition surface created by the scouring action of increased water flow velocity over underlying sediments. Located above the scour surface, previously scoured argillaceous debris and gravel tend to accumulate within scoured ditches and troughs (Figures 3d, 3e, and 3h).

(3) Cross bedding: Cross bedding is characterized by inclined laminae intersecting obliquely with bedding planes. This phenomenon can be further classified into tabular, wedge-shaped, trough-shaped, and pinnate cross bedding, based on the shape and characteristics of the laminae and the upper and lower interfaces. Tabular cross bedding is distinguished by parallel boundaries between laminae and a tabular shape. These features commonly manifest in sedimentary environments characterized by strong hydrodynamic conditions. On the other hand, Feathery cross bedding exhibits opposing dip directions of adjacent laminae within different layer systems, creating a feather-like appearance. Feathery cross bedding predominantly develops in tidal environments, characterized by the intersection of laminae at the boundaries of layer systems (Figures 3f and 3i).

(4) Parallel bedding: Parallel bedding is characterized by linear laminae that run parallel to each other. This type of bedding is commonly observed in coarse-grained sandstones, while horizontal bedding is more prevalent in argillaceous rocks and siltstones. Strong hydrodynamic forces, shallow water depths, fast flow velocities, or repeated scouring events are typically associated with the formation of parallel bedding. These conditions are often found in sedimentary environments with pronounced hydrodynamic activity.

(5) Flaser bedding: Flaser bedding refers to sediments composed primarily of sand, with thin and undulating mud layers or slender mud streamers intercalated within the sandy sediment when viewed in cross section. Flaser bedding is primarily developed in tidal environments, which are characterized by the alternation of marine and terrestrial influences (Figure 3j).

(6) Wavy bedding: Wavy bedding is characterized by a bedding interface that exhibits wave-like undulations. These undulations can be symmetrical or asymmetrical, regular or irregular. The wavy pattern generally aligns parallel to the bedding plane. Wavy bedding forms due to oscillatory hydrodynamic conditions and is predominantly developed in tidal environments, where regular fluctuations between high and low tides occur (Figures 3j and 3k).

Based on the analysis of sedimentary profiles and logging response characteristics, it can be inferred that the Benxi Formation is primarily composed of tidal flat-lagoon deposits that were obstructed by barrier islands (Wang et al., 2020; Liu et al., 2021; Radwan, 2021, 2022).

(1) The tidal flat facies in the Benxi Formation is primarily characterized by a combination of sandstone and mudstone. The gamma ray (GR) response is dominated by high-amplitude box, bell, toothed bell, and low-amplitude linear mud flat patterns. The sequence stratigraphy displays a pattern where mudstone or coal seams are positioned below the sequence boundary, followed by tidal channel sedimentary sandstones above the boundary, and one or more upward fining retrograding parasequences. Microfacies such as sand flats, mud flats, and tidal channels are prominent within this facies (Figure 4).

(2) In the mixed tidal flat area characterized by a combination of sand, mud, and limestone, the GR data exhibits characteristics of lime flats and mud flats, displaying middle-amplitude toothed bell shapes, high-amplitude toothed box shapes, and low-amplitude linear shapes. Sequence analysis reveals the presence of sandstones and mudstones below the sequence boundary, while mixed sedimentary limestone is observed above the boundary. Microfacies such as mixed flats, mud flats, tidal channels, and sand flats are well-developed within this facies (Figure 4).(3) Within the mixed lagoon area dominated by limestone and mudstone, the GR data showcases a combination of high-amplitude dentate box-shaped, low-amplitude tongue-shaped, linear limestone flat patterns, and lagoon mud. Sequence analysis indicates that lagoon mudstone resides below the interface, with mixed lagoon-deposited limestone positioned above the interface. Prominent microfacies within this facies include limestone flats and mud flats (Figure 4).

4.2.2. *Distribution characteristics of sedimentary facies*

Different interpretations regarding the division of sedimentary facies in the Gaoqiao area have been proposed by previous researchers, who considered the specific conditions of their respective study areas. Consequently, the classification of sedimentary facies in the Gaoqiao area remains a subject of ongoing debate. For instance, Feng et al. (2021) categorized the area as a barrier coast sedimentary system, showing a progression from barrier bars to lagoons. They identified three primary detrital sedimentary units: subtidal to exposed surface barrier

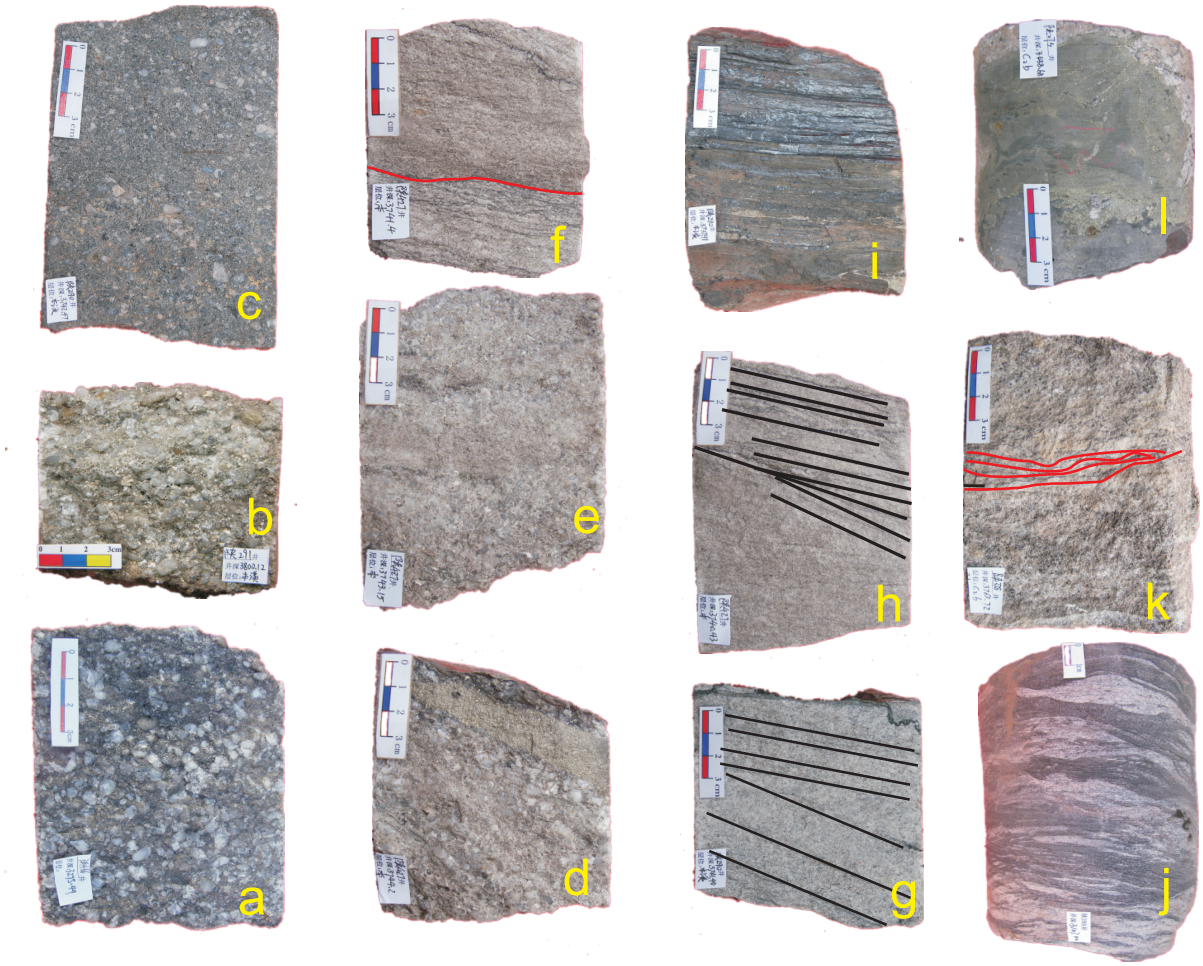

Figure 3. a. Gray quartz conglomerate, well S466,3276 m; b. quartz conglomerate,well S291, 3800 m; c. gray gravelly coarse sandstone, well S290, 3742.47 m; d. conglomerate, fine sandstone, developed pyrite nodules, well S427, 3744.2 m;e. gray white quartz sandstone, well S427, 3743.15 m;f. gray sandstone, developed plate-like oblique bedding, low angle cross bedding, well S290, 3741.40 m;g. sandy bedding, well S338, 3739.4 m; h. sandy bedding, weak scouring surface, well S427, 3741 m;ı. platy bedding is developed, and the bedding surface is rich in carbon,Well S427, 3740.43 m; j. flaser bedding, well S289, 3105 m; k. Mudstone tearing structure with pyrite nodules developed, well S273, 3438 m;l. Carbonaceous siltstone, well S290, 3737 m.

bars, lagoons, and clastic tidal flats (Feng et al., 2021). The presence of a tidal flat-barrier island sedimentary facies can be attributed to seawater intrusion from the east to the west, towards the central ancient uplift. On the other hand, Hou et al. (2018) focused on the central and southern regions and proposed a composite sedimentary model that experienced transformations due to strong tides while still maintaining the morphological characteristics of a delta (Hou et al., 2018).

The Benxi Formation in the Ordos Basin is a sedimentary unit that has undergone extensive weathering and denudation over a long period (Li et al., 2014). Due to its filling characteristics, the formation's thickness varies across different locations. Specifically, it exhibits greater thickness in lowlands, depressions, gullies, and troughs, while thinner thickness is observed in highland and low protuberance areas. The upper section of the formation comprises grayish black/gray mudstone, siltstone, and other sediment types. Within this horizon, unstable thin coal seams or coal lines can be intermittently found. Notably, the distribution of thin limestone lenses in the middle section of the Benxi Formation varies significantly. While limestone is distinctly absent in the western portion of the study area, it is found in a substantial deposit in the east.

According to the sediment assemblage in the study area, three main types of tidal flats can be identified from west to east: clastic tidal flat, mixed tidal flat, and mixed lagoon. Among these, the clastic tidal flat is the predominant type.

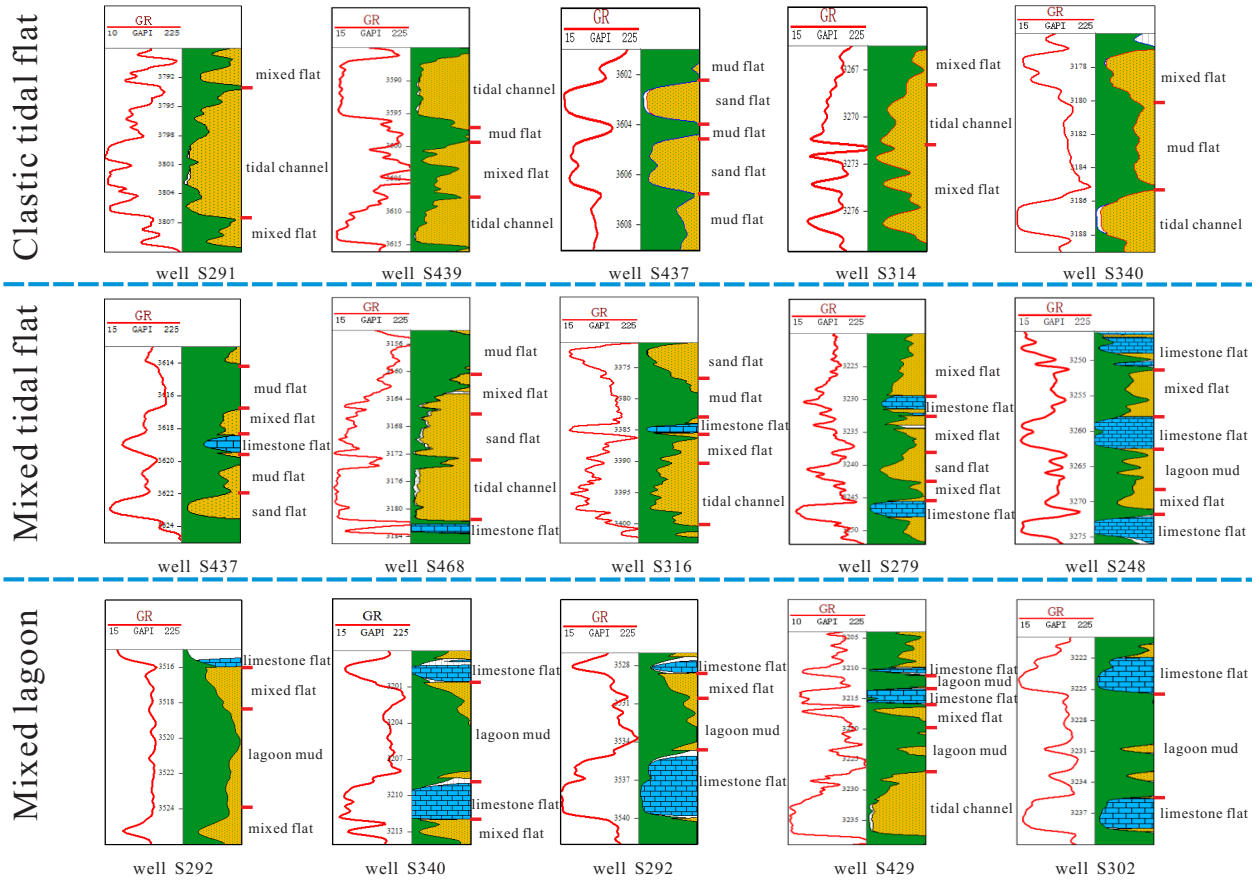

Figure 4. Logging response and lithologic association characteristics of three typical sedimentary facies belts (clastic tidal flat, mixed tidal flat and mixed lagoon) in Benxi Formation.

(1) The sediments found in the clastic rock tidal flat mainly consist of claystone, siltstone, and fine sandstone. On a horizontal plane, the grain size of sediments shows a gradual transition from coarse to fine when moving from east to west. Based on the distribution characteristics of plane lithology, this type of tidal flat can be further divided into sand flat, mixed flat deposits, and a few mud flats (Figures 5 and 6).

To the west of the line running through wells S100, G65-9, S338, S290, G74-11, G79-21, and S318, the sand flat deposits of the Benxi Formation primarily consist of grayish-white fine sandstone, pebbly unequal sandstone, and light gray siltstone. These sediments also contain a small amount of carbonized plant debris and other argillaceous deposits. The sandstone exhibits moderate sorting and poor rounding, with the presence of sand cross bedding. The thickness of the sand layers varies from 2 to 15 m. The grain size gradually transitions from coarse sandstone to medium-coarse sandstone from the bottom to the top, forming a vertical sequence of pinnate cross bedding, trough cross bedding, and ripple bedding.

Mud flat deposits can be observed between the sand flats and primarily consist of thick argillaceous deposits, such as mudstone, silty mudstone, and shale. In some areas, thin layers of lenticular siltstone and coal seams are intercalated within these deposits. The sedimentary structure of the mud flats is mainly characterized by horizontal laminae.

(2) The mixed tidal flat in the study area is characterized by sediments primarily composed of conglomerate, sandstone, mudstone, and limestone. Within this tidal flat, the main features that are developed include east-west tidal channels, mixed flat deposits, and marsh sediments (Figures 5 and 6).

Tidal channels, as extensions of the tidal range, represent high-energy hydrodynamic environments. The sediments found within these channels consist of grayish-brown medium-fine quartz conglomerate and coarse

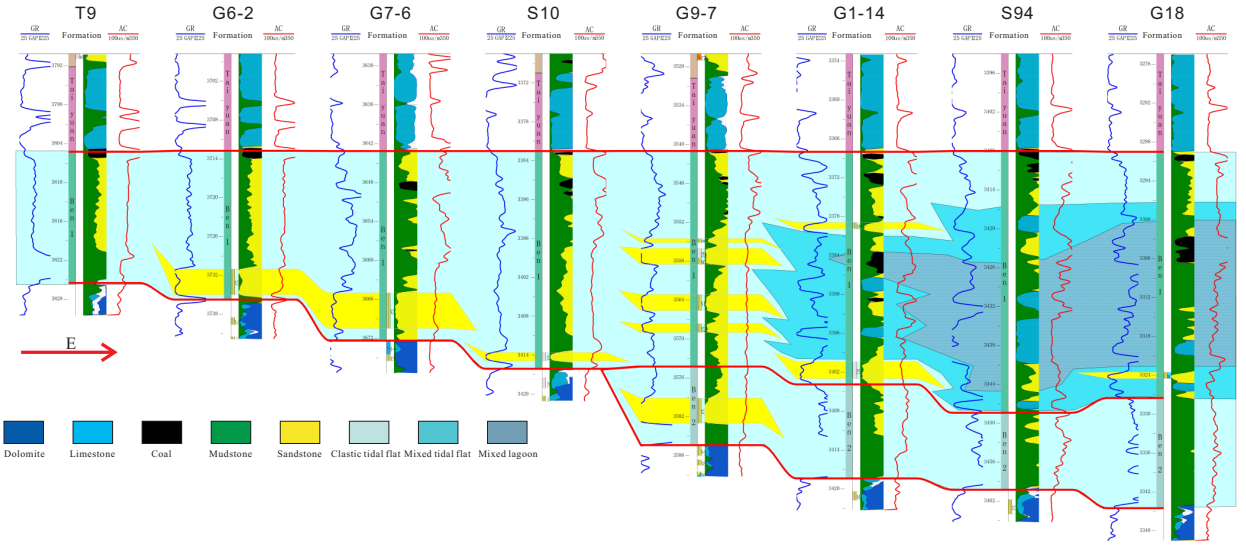

Figure 5. Cross section of sedimentary facies of Benxi formation from well T9 to well G18 (profile 1 in Figure 7).

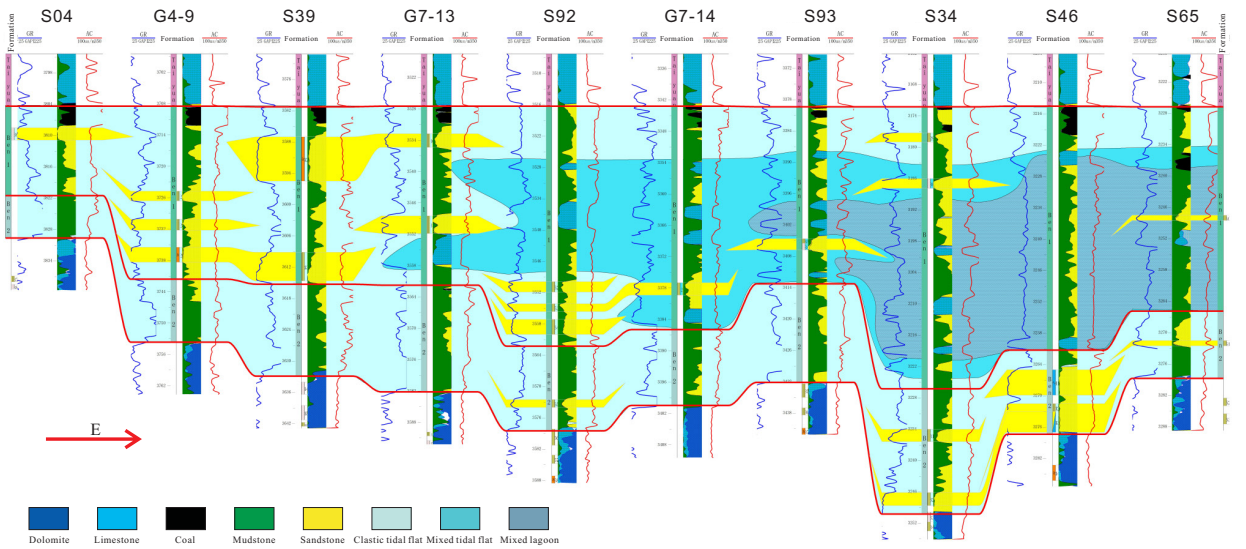

Figure 6. Cross section of sedimentary facies of Benxi formation from well S04 to well S65 (profile 2 in Figure 7).

sandstone with a high quartz content. The sedimentary structure is dominated by pronounced trough cross bedding and bidirectional pinnate cross bedding. Well-defined scour surfaces, along with lag deposits and visible mud gravel, are present at the bottom of the channels. Multiple tidal channels can be vertically stacked, resulting in a superimposed pattern of trough cross bedding, pinnate cross bedding, mudstone, tabular cross bedding, and mudstone.

Mixed flat deposits are primarily composed of thin interbeds of sandy rock and argillaceous rock, occasionally intercalated with limestone and argillaceous limestone. As hydrodynamic conditions weaken from the bottom to the top of the mixed flat deposit, the mud content gradually increases. This change in sediment composition often results in vein bedding, wavy composite bedding, and lenticular bedding. The typical vertical lithofacies sequence within the mixed flat deposit includes tidal bedding siltstone

facies, ripple bedding siltstone facies, and tidal bedding silt sandstone facies, with tidal bedding silt sandstone facies being the most common.Marshes play a significant role as sedimentary environments within the tidal sedimentary system, specifically in the supratidal zone. The continuous ebb and flow of tides create favorable conditions for the formation of extensive vegetation in certain areas, thus promoting marsh development. The marsh sediments of the Benxi Formation are predominantly gray-black and black mudstone, containing a significant number of plant fossils. Coal seams are commonly observed within these deposits.

(3) The mixed lagoon, observed in the northeast part of the study area and east of the line running through S137, S96, S475, and G23-103, represents a semienclosed water area that is either connected to the open sea through tidal channels or in a semiisolated state. This lagoon exhibits shallow water depths and low hydrodynamic conditions (Figures 5 and 6).

The predominant lithology within the mixed lagoon consists of grayish-black and dark gray mudstone, carbonaceous mudstone, and coal seams. These strata are occasionally interbedded with thin layers of siltstone, argillaceous siltstone, or fine sandstone. Plastic deformation bedding and horizontal laminae are common features found within the interbedding of sandstone and mudstone. The limestone found in the area is predominantly gray-black micrite limestone, often containing calcite-filled shell fossils. The presence of pyrite within the core suggests a reduced sedimentary environment.

During the deposition of the Benxi period, significant geological events occurred that influenced the sedimentary environment in the study area. Firstly, there was stress exerted in the east-west direction, resulting in a gradual subsidence of the basement. This subsidence was accompanied by a rise in sea level, creating favorable conditions for sediment deposition. Towards the end of the Benxi period, there was a rapid decline in sea level, leading to the formation of a stable swamp environment.

In comparison, during the deposition of the Ben 1 member, there was an overall rise in sea level, accompanied by further basement subsidence. This period also witnessed the expansion of the North China Sea, which intruded westward (northwestward). As a consequence of these geodynamic changes, the entire barrier coast depositional system was shifted westward. Consequently, during the sedimentary period from the Ben 2 to Ben 1 member, the littoral-neritic sea in the study area continuously expanded its range. The boundaries between the littoral-neritic sea and the barrier-lake, as well as the boundary between the barrier-lake and the tidal flat, both moved westward (Figure 7).

In the western part of the study area, a central paleo-uplift extends in a north-south direction, while to the east lies the North China Sea. The proximity of the paleo-uplift to the North China Sea has resulted in the formation of tidal flat deposits influenced by tidal action. Based on the analysis of lithological associations, sedimentary facies sequences, and their distribution, it is evident that within the study area, the Benxi Formation is primarily characterized by terrigenous clastic rock deposits. Additionally, there are occurrences of mixed strata comprising both terrigenous clastic rocks and carbonate rocks, which are vertically stacked upon each other. The sedimentary environment within the study area transitions from west to east, encompassing clastic tidal flat, mixed tidal flat, and mixed lagoon facies. The mixed lagoon is predominantly developed in the northeastern part of the study area, while the mixed tidal flat is distributed in a ring belt around the lagoon (Figure 7) to the east.

4.3 Petrological characteristics

Within the study area, the Benxi Formation exhibits a range of sandstone components. The relative quartz content in the sandstone varies from 65% to 100%, with an average of approximately 88%. Conversely, lithic debris constitutes 3% to 35% of the sandstone, with an average content of about 15%.

Concerning compositional maturity, the Q/(F+R) ratio is notably high, indicating a prevalence of mature sandstones. The predominant sandstone type primarily is quartz sandstone (Figure 8).

The rock components within the studied area encompass clay minerals and cements. Notably, the cements predominantly consist of authigenic quartz and dolomite. Authigenic quartz is observed as well-formed euhedral crystals within the intergranular pores, along with localized quartz overgrowth (Figures 9a–9d).

As for the clay minerals, they are primarily represented by kaolinite and illite (Figure 9c–9f). Local occurrences of chlorite are also observed. Kaolinite is observed within intergranular pores, displaying a morphology reminiscent of pages or worm-like structures. The development of kaolinite in some areas leads to a reduction in overall pore space. However, its development of intergranular pores contributes to an increase in pore space. Illite and chlorite, however, form a coating film around clastic particles, although their overall degree of development is comparatively low.

4.4 Porosity, permeability and pore structure

4.4.1 *Physical characteristics*

The physical properties of tight sandstone reservoirs play a crucial role in determining their overall reservoir properties and productivity. Based on core testing, the porosity of the Benxi Formation sandstone is observed to range from 2.29% to 12.73%, with an average porosity of

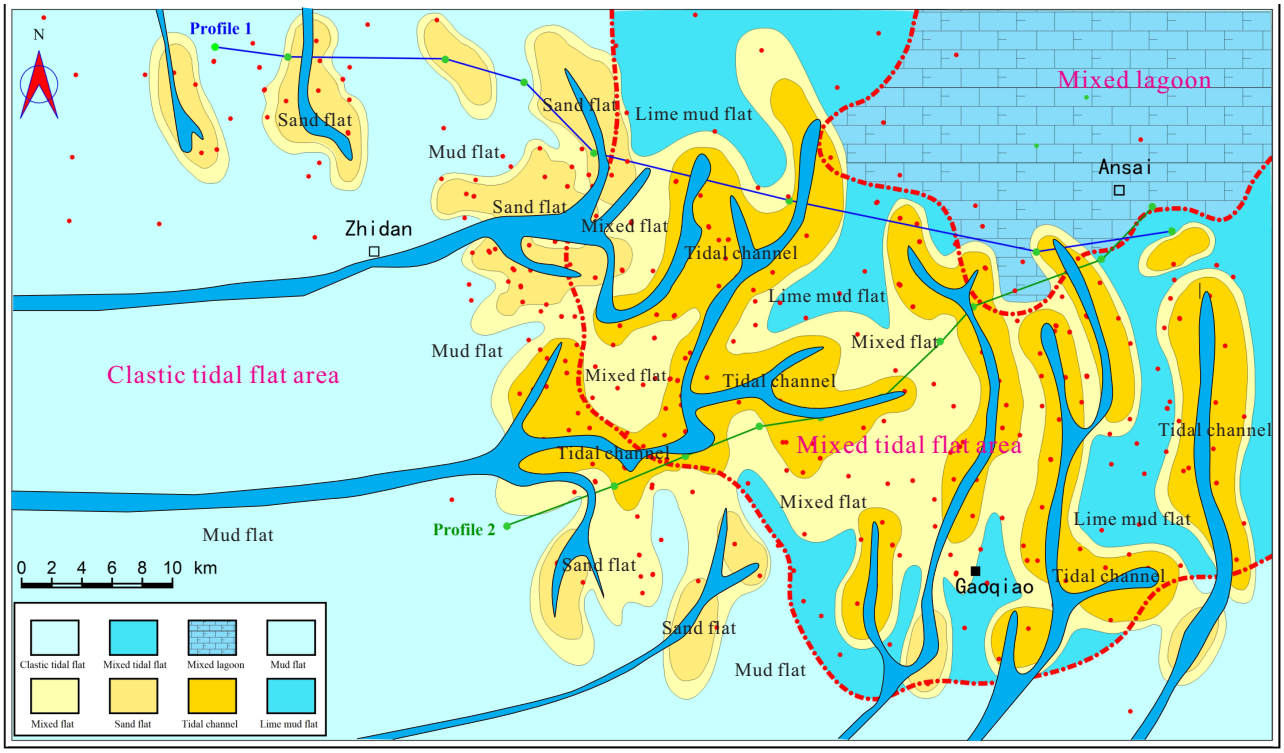

Figure 7. Sedimentary facies map of Benxi Formation in the Gaoqiao area (study area in Figure 1).

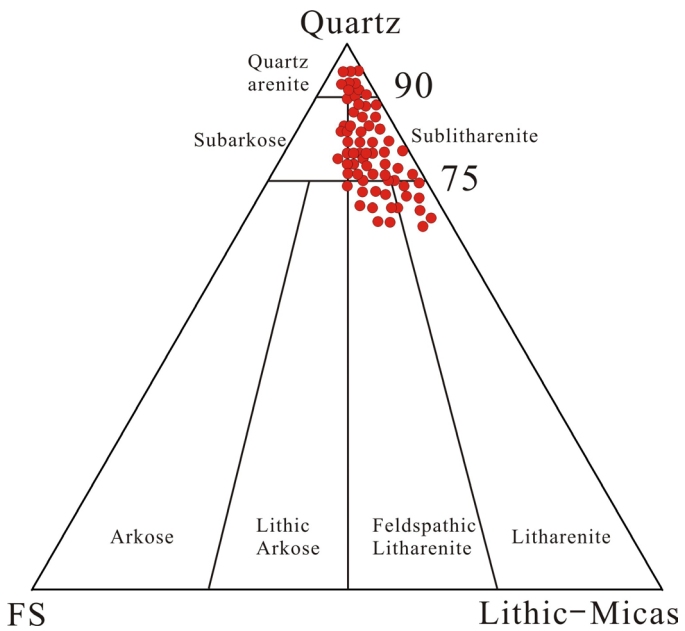

Figure 8. Sandstone type triangular diagram of the Benxi Formation Gaoqiao area (classification according to Folk (1980)).

6.36%. This indicates a generally low porosity characteristic of the reservoir.

Furthermore, the permeability of the sandstone is observed to range from 0.07 mD to 43.55 mD. Notably, over 75% of the samples exhibit permeability values below 10 mD, further emphasizing the low permeability nature of the reservoir. On average, the permeability is measured to be 1.9 mD, indicating limited fluid flow capability.

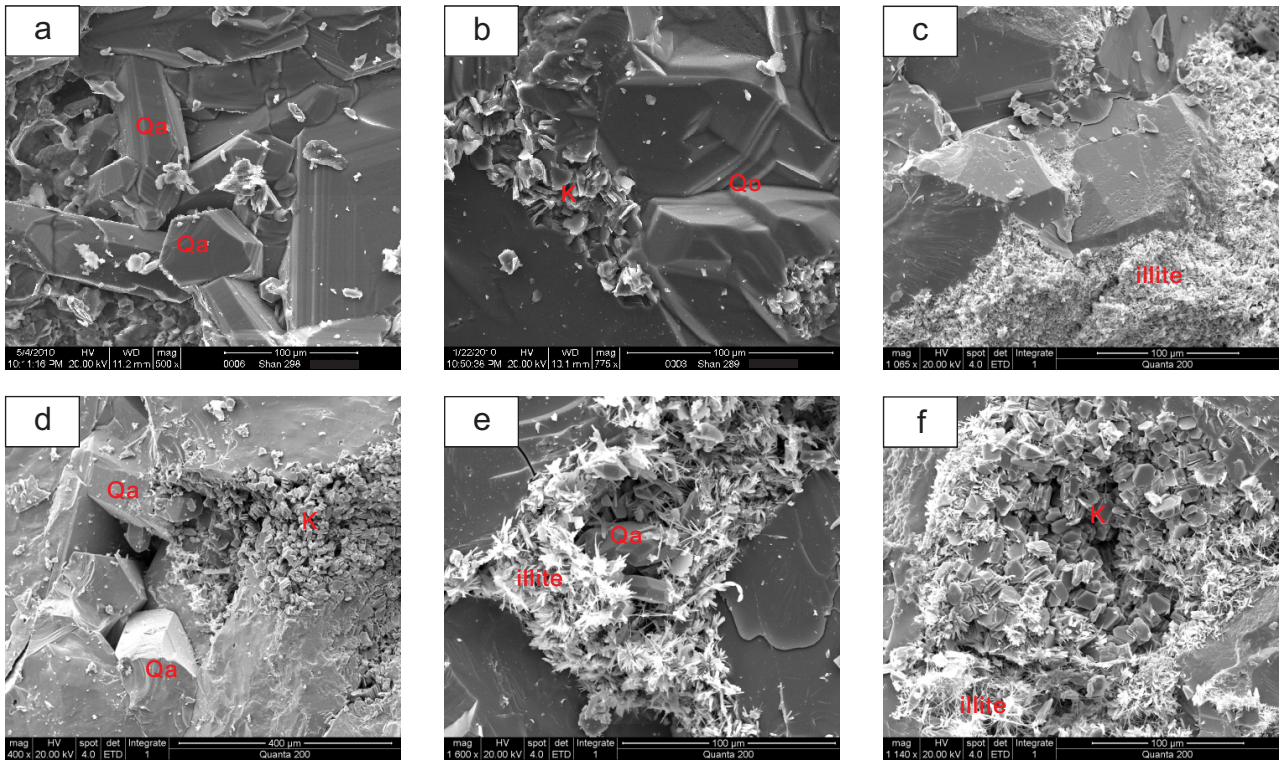

Figure 9. SEM images showing typical cement habits and dissolution of Benxi sandstones: a. the authigenic quartz cementation in intergranular pores is developed, with a high degree of automorphism, well S289, 3105.48 m; b. quartz overgrowth and kaolinite cemented filling pores, well289, 3105.48 m; c. sandstone is dense, and the surface of clastic particles is commonly illitized, well S318, 3212.94 m; d. quartz cementation develops in intergranular pores, and local clastic dissolution forms kaolinite, well S465, 3183.73 m; e. lamellar illite cemented intergranular pores, well S366, 3827.62 m; f. kaolinite coexists with illite, cementing pores, well S466, 3278.71 m.

Given the limited number of cored wells available for the Benxi Formation in the study area, this research focuses on comparing the physical properties of the two members to better understand the reservoir characteristics within the formation. The analysis primarily relies on experimental test results and the interpretation of physical properties derived from logging data. The objective is to identify efficient reservoir characteristics, with a particular emphasis on discerning differences in reservoir properties under various depositional modes.

To accomplish this, it is necessary to expand the scope of correlation beyond individual depth measurements to encompass the average physical properties of one or several continuous sandstone bodies in the vertical direction. By doing so, a more comprehensive assessment of the collective influence of sedimentary models on reservoir development can be attained.

A comparative analysis reveals a general consistency between the scale physical properties of sandstone bodies within the Ben 1 and Ben 2 members and the results obtained from experimental testing. However, since physical property values represent mean values, they tend to be relatively small overall. Porosity is primarily distributed within the range of 2% to 6% (Figure 10a), while permeability is predominantly distributed within the range of 0.01 mD to 0.4 mD (Figure 10b).

The porosity of individual sandstone bodies within the Ben 1 formation exhibits a distribution spanning from 0.09% to 9.25%, with an average value of 3.88%. Permeability values range from 0.01 mD to 3.72 mD, with an average value of 0.29 mD. Notably, 26.6% of the sandstone bodies in the Ben 1 formation are considered effective as they possess porosity values exceeding 5% (Figure 10c).

For the sandstone bodies within the Ben 2 formation, porosity ranges from 0.10% to 8.62%, with an average value of 3.43%. Permeability ranges from 0.01 mD to 5.21 mD, with an average value of 0.25 mD. Within the Ben 2 formation, 19.7% of the sandstone bodies are classified as effective due to having a porosity exceeding 5% (Figure 10c).

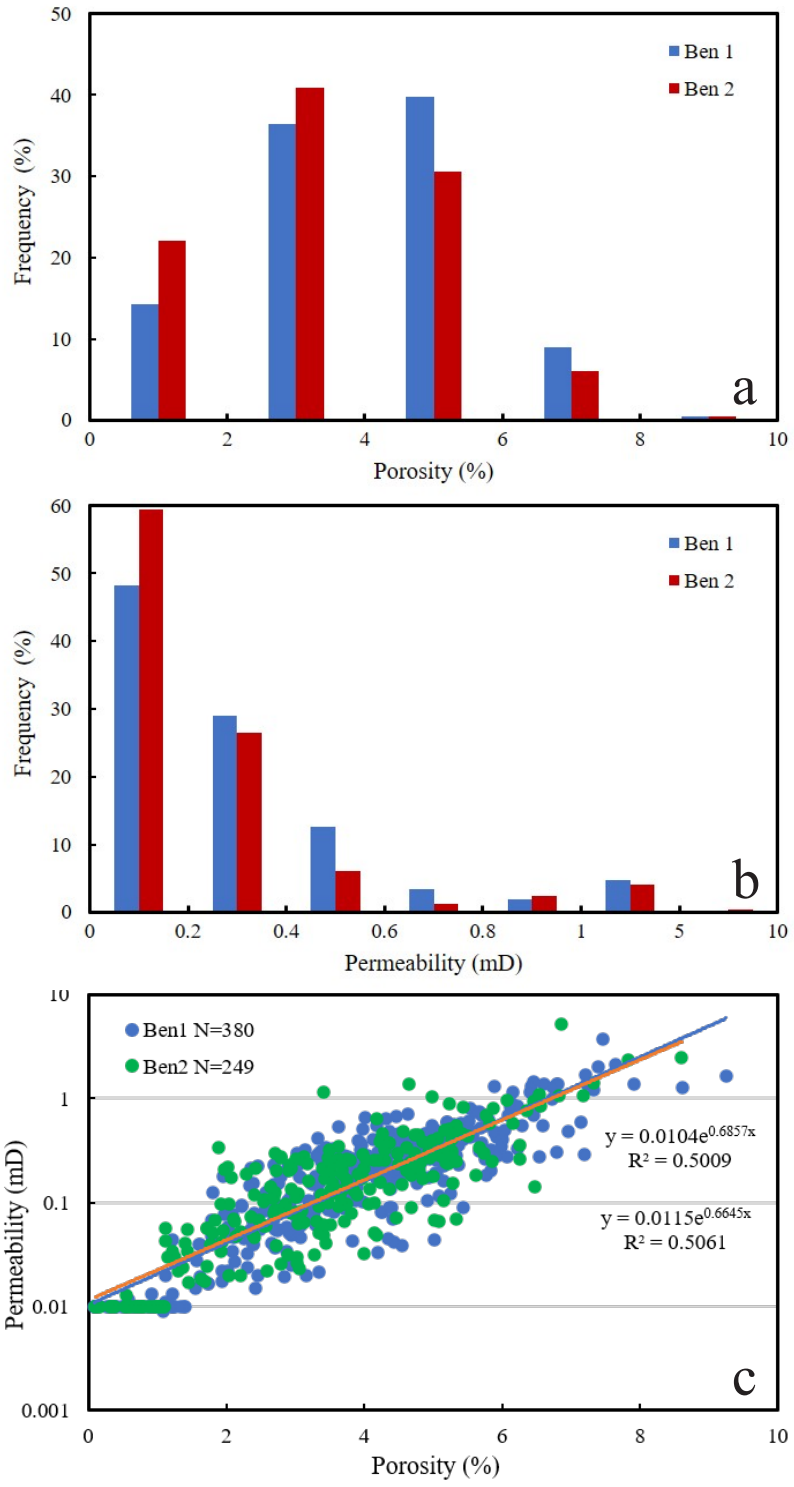

Figure 10. Reservoir physical properties of the sandstone of Benxi Formation: a. porosity distribution; b. permeability distribution; c. porosity versus permeability plot.

While the physical properties of the sandstone within the Ben 1 formation generally display slightly higher values compared to those within the Ben 2 formation, a strong exponential correlation is observed between the porosity and permeability of both intervals. This suggests that an increase in porosity tends to correspond to a proportional increase in permeability, reflecting a consistent relationship between these two properties.

4.4.2. ***Pore structure characteristics***

High-pressure mercury injection and microscopic imaging techniques offer distinct advantages in characterizing the pore structure of tight sandstone. High-pressure mercury injection is particularly useful for investigating pore size, distribution, the geometry of pore throats, and pore throat connectivity within the tight sandstone. On the other hand, microscopic images provide valuable insights into the spatial configuration and morphology of the pores.

By employing high-pressure mercury injection, researchers can analyze the pore structure of tight sandstone in terms of its size distribution, the overall geometry of pore throats, and the connectivity between them. This technique allows for a detailed examination of the intricate network of pores present in the rock. Complementarily, microscopic imaging provides visual evidence of the sandstone's pore structure at a microscale, aiding in the identification and characterization of specific pore types and their spatial arrangements.

The predominant pore types observed within the sandstones of the Benxi Formation primarily consist of dissolution pores originating from feldspar and rock debris, as well as early residual primary intergranular pores (Figure 11). Other pore types and microfractures are relatively poorly developed. The distribution of pore diameter typically ranges from 10 μm to 200 μm, with the majority of pores having diameters less than 100 μm, classifying them as micromesopores. Pore throats predominantly display flaky and necked characteristics. The porosity distribution on the lower surface of the microscopic sheets generally ranges from 2% to 8%. Based on the combination of pore types and structural characteristics, the sandstone can be categorized into three main types (Figure 12).

1. Primary intergranular pore type

The analyzed sandstones exhibit a relatively high quartz content, with some samples displaying a developed chlorite rim at the grain edge. The predominant pore type is residual primary intergranular pores. Following diagenetic transformations such as compaction, pressure solution, and cementation, the residual intergranular pores typically assume angular shapes, often resembling irregular triangles or quadrangles (Figure 11a). The pore connectivity within these sandstones is notably robust. Image analysis reveals a distribution of pore equivalent diameter ranging from 5 μm to 80 μm. Pores within the

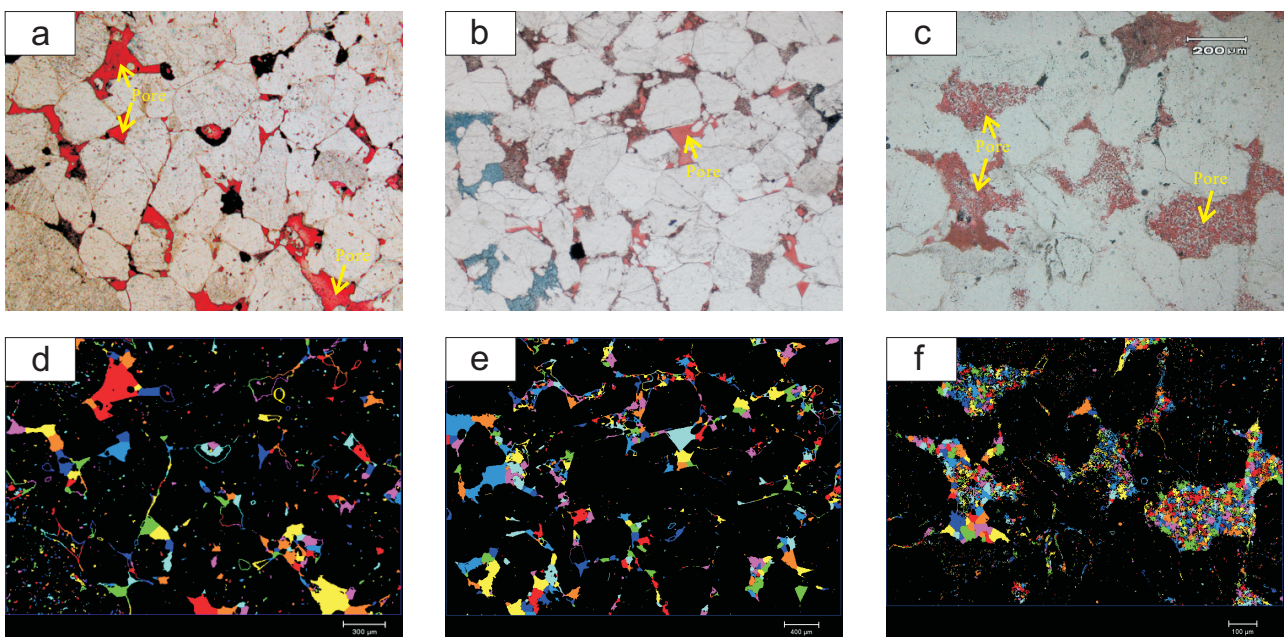

Figure 11. Pore structure characteristics of three typical pore sandstones in Benxi Formation. a. pore characteristics in microscopic slices; b. pore characteristics extracted and segmented by software; c. distribution characteristics of pore quantity in different equivalent pore diameter intervals; d. distribution characteristics of pore area in different equivalent pore diameter intervals.

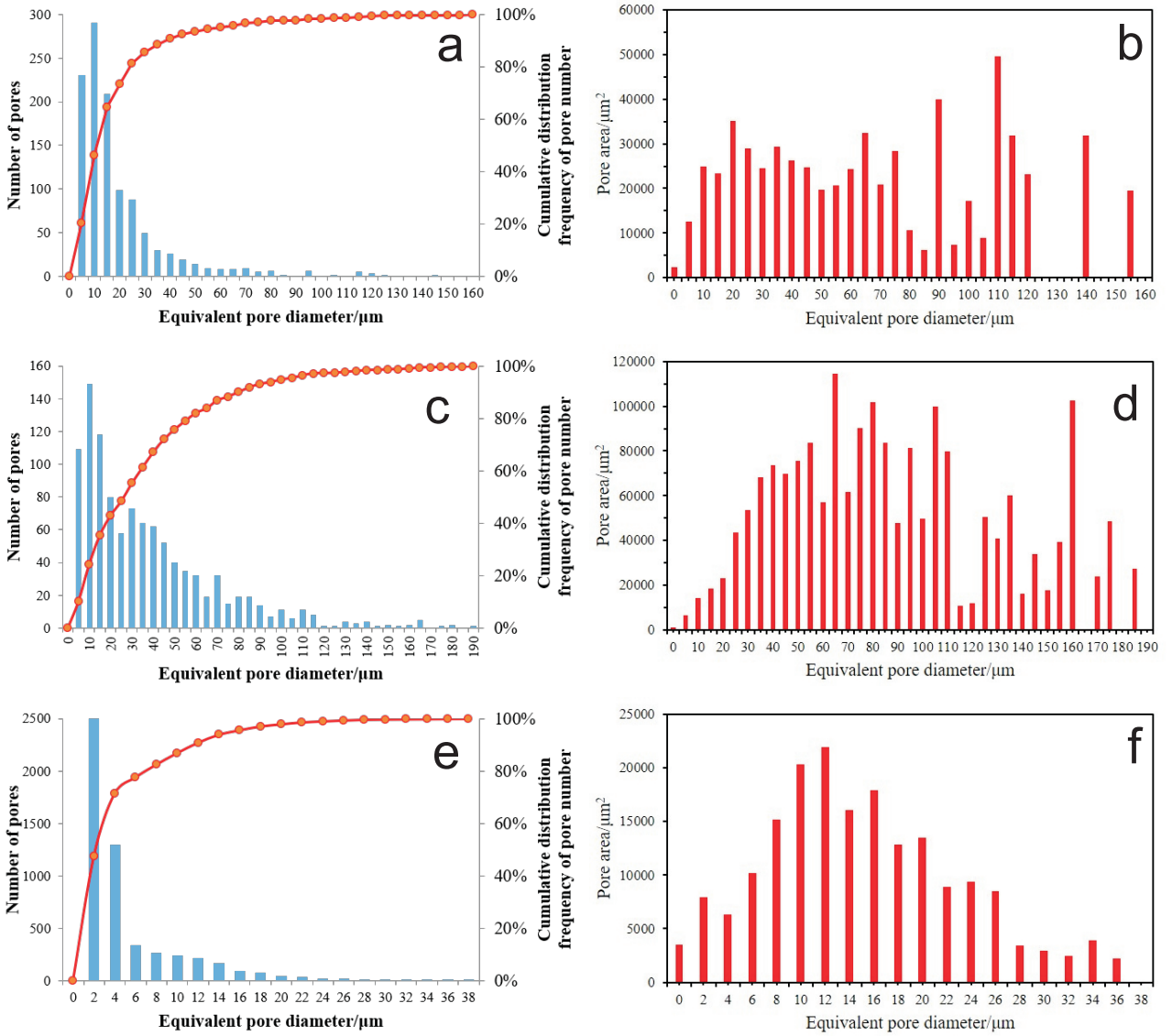

Figure 12. Pore structure characteristics of three typical pore sandstones in Benxi Formation. a. pore characteristics in microscopic slices; b. pore characteristics extracted and segmented by software; c. distribution characteristics of pore quantity in different equivalent pore diameter intervals; d. distribution characteristics of pore area in different equivalent pore diameter intervals.

5 μm to 20 μm range demonstrate the highest frequency, while pores within the 20 μm to 80 μm range contribute significantly to surface porosity (Figures 12a and 12b).

High-pressure mercury injection analysis demonstrates that the porosity of this sandstone type generally exceeds 8%. Permeability, however, varies considerably depending on the degree of compaction and cementation, with values ranging from 0.25 mD to 5.1 mD. The median pore radius surpasses 0.5 μm, while the displacement pressure ranges from 0.5 MPa to 1.2 MPa. The maximum mercury saturation exceeds 85%, but there are a few samples where saturation is below 50% (Figure 13a).

2. Dissolution pore and primary pore combination type

The residual primary intergranular pores in this sandstone exhibit relatively small diameters, often hosting quartz and dolomite cements. Various types of dissolution pores are observed, primarily including lithic and feldspar marginal dissolution pores, as well as intergranular dissolution pores. Marginal dissolution pores are formed at the grain edge of residual primary intergranular pores and may exhibit harbor-shaped, concave-convex, or serrated geometries. Additionally, intragranular dissolution pores and moldic pores are also present. Concerning intragranular dissolution, quartz components show less developed

pore structures, while feldspar particles exhibit more pronounced intragranular dissolution pores (Figure 11b). Overall, there is relatively good connectivity among the pores, particularly in relation to dissolution development, contributing to the formation and development of throats to some extent. Based on image analysis, the distribution of pore equivalent diameter primarily falls within the range of 5 μm to 50 μm, with a peak number of pores observed within the range of 5 μm to 20 μm. However, pores in the range of 25 μm to 80 μm significantly contribute to the overall surface porosity (Figures 12c and 12d).Analysis using high-pressure mercury injection indicates that this type of sandstone typically exhibits porosity ranging from 5% to 9%. Permeability values range from 0.1 mD to 1 mD. The median pore radius ranges from 0.2 μm to 1.2 μm, and the displacement pressure varies between 0.6 MPa and 1.8 MPa. The maximum mercury injection saturation ranges from 65% to 80% (Figure 13b).

3. Dissolution pore is the main type

The pore structure of this particular sandstone predominantly consists of dissolution pores. Due to the high intensity of dissolution processes, intragranular dissolution pores are prevalent within feldspar and debris, along with a limited number of dissolution pores. Notably, in sandstones with well-developed feldspar, the presence of kaolinite is often observed as a result of dissolution. This, in turn, leads to weakened internal pore connectivity influenced by clay minerals (Figure 11c).

The distribution of pore equivalent diameter is primarily within the range of 2 μm to 14 μm, with the largest contribution to surface porosity observed within the range of 6 μm to 26 μm (Figures 12e and 12f).

High-pressure mercury injection analysis reveals that the porosity of this specific type of sandstone generally falls below 7%. The main characteristics of this sandstone include the development of dissolution pores in conjunction with the presence of clay minerals. Additionally, the permeability of this sandstone type is significantly lower compared to the first two types discussed. The median pore radius ranges from 0.05 μm to 12 μm, with a displacement pressure ranging from 0.8 MPa to 3.5 MPa. The maximum mercury saturation is typically less than 70%, with only a few samples exceeding 80% saturation (Figure 13c).

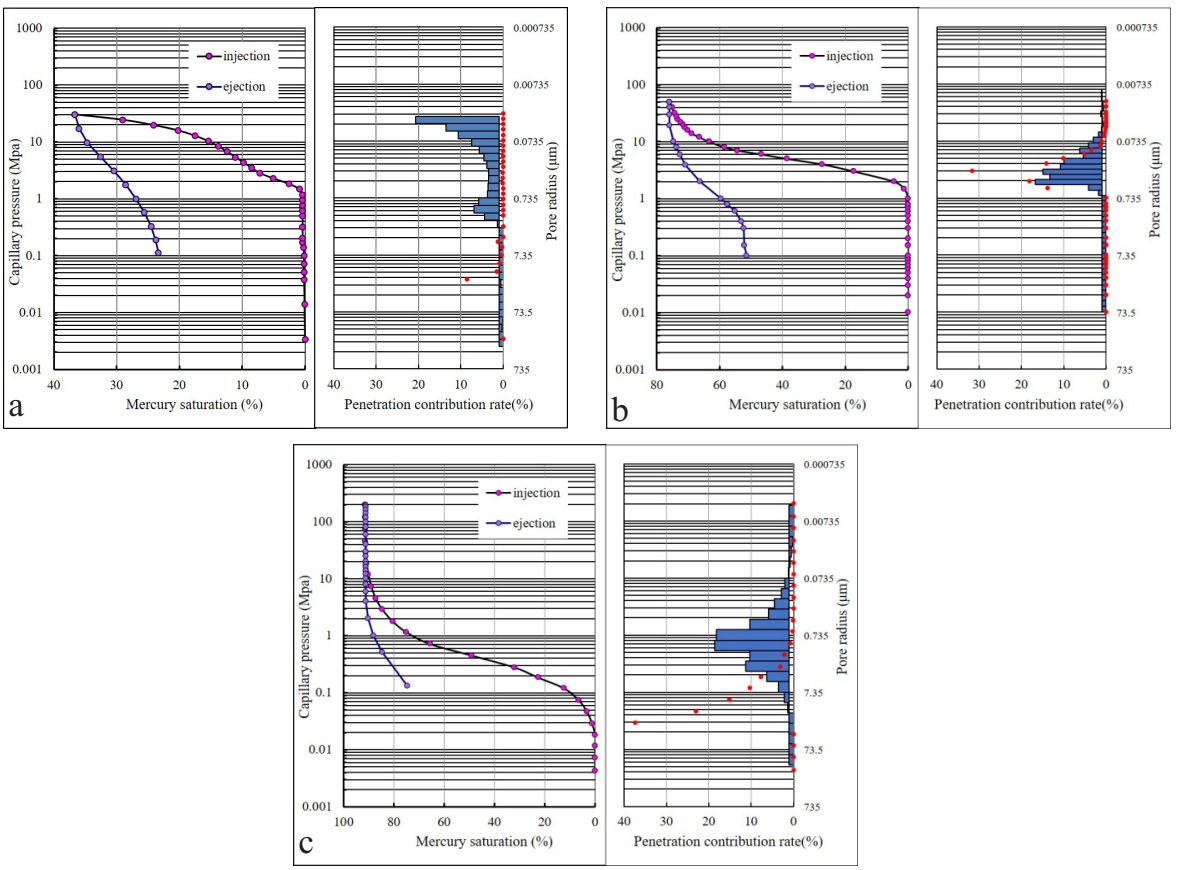

Figure 13. Capillary pressure curve and pore throat radius distribution from high pressure mercury injection analysis of Benxi Formation sandstone in Gaoqiao area.

In general, the reservoir sandstones within the studied area predominantly exhibit characteristics of type 2 and type 3 sandstones. Notably, the high-yield intervals observed within the Ben 1 member are primarily associated with the development of type 1 and type 2 sandstones. This observation underscores the significant relationship between the efficiency of reservoir development in generally tight sandstones and the extent of residual primary intergranular pore development. As a result, this research focuses on examining the interrelationship.

The primary pores within the Benxi Formation display varying degrees of development among different wells. These pores exhibit pronounced dissolution effects, leading to the development of intergranular dissolution pores, intragranular dissolution pores, and intergranular diffusion pores. Upon analyzing the pore structure of the sandstone within the Benxi Formation, it is noted that the reservoir section displays a high degree of pore development. Additionally, strong connectivity is observed among the primary pores.

4.5 Diagenesis and authigenic mineralogy

The results from thin section observation and scanning electron microscope analysis reveal that diagenesis in the study area is complex, with a plethora of diagenetic phenomena occurring in the sandstone. The primary diagenetic processes observed include compaction, cementation, and dissolution.

The discharge of intraformational water and pore water, induced by overlying gravity and hydrostatic pressure, leads to the close arrangement of clastic grains and a reduction in pore volume and porosity. This reduction in porosity and permeability significantly contributes to the low-quality characteristics of the sandstone reservoirs (Bjørlykke, 2014; Wang et al., 2017; Wang et al., 2019a, 2019b). The grains exhibit linear and concave-convex contacts, indicating compaction predominantly through the plastic deformation of soft components such as volcanic debris, mudstone debris, mica, and schist debris (Wang et al., 2022). On average, compaction results in a 25% loss of primary porosity. Some samples also display linear and suture contacts between quartz particles and debris particles, caused by pressure solution.

Cementation, another diagenetic process contributing to the compactness of sandstone , involves the precipitation of authigenic minerals from pore fluids that act as binding agents, thereby consolidating loose sediments. The Benxi Formation exhibits various cements resulting from changes in the diagenetic environment. These include siliceous cement, carbonate cement (dominated by ankerite in continuous or mosaic crystal forms), and clay mineral cement. Siliceous cementation is prominent during the early stages and manifests as quartz secondary enlargement, altering particle contacts, blocking pore throats, and reducing the reservoir's percolation capacity with significant destructiveness. Clay minerals, either through internal lining or particle coating, contribute to the reduction of microscopic seepage capacity of pores (Bjørlykke, 2014).

Dissolution is a crucial diagenetic mechanism that generates secondary pores and enhances the physical properties of reservoirs in the area. Dissolution primarily takes place within clastic particles, such as feldspar, rock debris, and parent rock, as well as interstitial materials, including calcite and clay, and individual clastic particles. Extensive dissolution leads to the formation of numerous pores and provides source materials for the formation of authigenic quartz, ferrocalcite, and other cements within secondary pores (Crundwell, 2014; Huang et al., 2020). The increment in porosity resulting from sandstone dissolution ranges from 0.3% to 8%, with an average of 4%. These dissolved pores account for over 60% of the total areal porosity, making them the most significant type of reservoir space.

To examine the reservoir development characteristics, the sandstones within the Benxi Formation Member were categorized into lithofacies based on distinct parameters such as sandstone clastic composition, diagenetic minerals, diagenetic type and strength, and pore structure (Wang et al., 2017; Wang et al., 2019a). The identified lithofacies are as follows:

A. Strong compaction facies (Figure 14a),

B. Strong compaction and strong cementation facies (Figure 14b),

C. Strong compaction, medium cementation, and weak dissolution facies (Figure 14c),

D. Strong cementation facies (calcite and dolomite) (Figure 14d),

E. Strong dissolution-primary pore development facies (Figures 14e and 14f).

Due to the combined effects of strong compaction and cementation, lithofacies A, B, and D exhibit a very low degree of sandstone pore development. Conversely, facies C and E possess the potential to develop into high-quality reservoirs, either through dissolution processes or primary pore development.

5. Discussion

5.1. Control of sedimentary on reservoir quality

The sedimentary environment plays a crucial role in determining the properties of reservoirs. It governs the original composition and structure of reservoir rocks, as well as the initial pore structure, thereby exerting a significant influence on subsequent diagenesis processes (Folk, 1980; Ehrenberg, 1990; Ng et al., 2019). The control of the sedimentary environment on the reservoir is reflected in the control of sedimentary facies belts

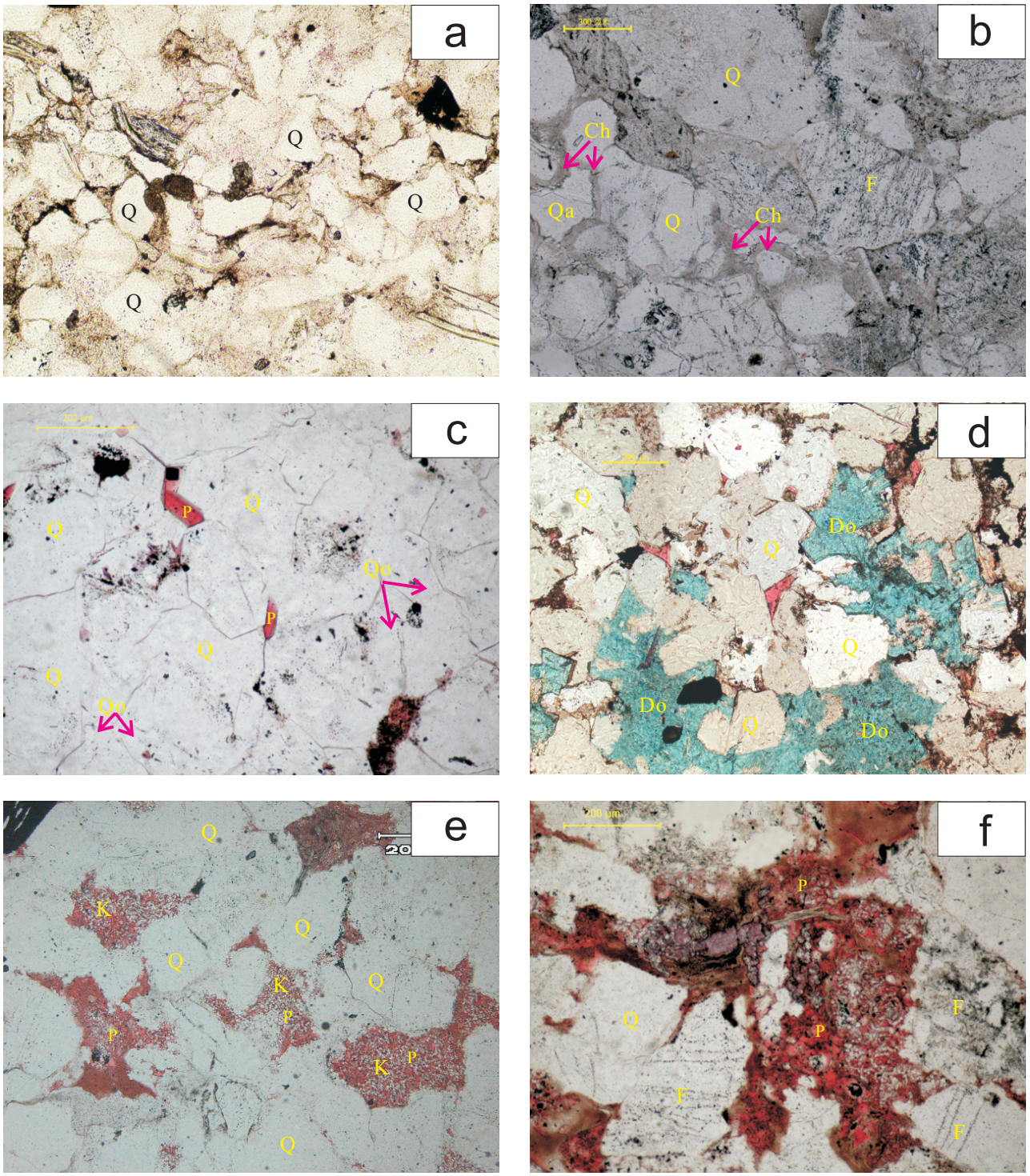

Figure 14. Photomicrographs under plane-polarized light showing pore structure and diagenesis in Benxi sandstones: a. strong compaction, undeveloped pores, well S426, 3384.20 m; b. strong compaction, strong quartz cementation, well S469, 3223.71 m; c. after strong compaction and medium cementation transformation, locally developed pores, well S289, 3105.87 m; d. dolomite strongly cemented, well S426, 3380.53 m; e. strong dissolution, pore development, well S291, 3799.21 m; f. development of solution pores and primary intergranular pores, well S427, 3740.98 m.

on the type and physical characteristics of sandstone bodies. Different sedimentary environments exhibit distinct sedimentary conditions and patterns, resulting in variations in the components and structures of sandstone bodies (Morad et al., 2010; Okunuwadje et al., 2020). In the Benxi Formation, sand flats and tidal channels are the dominant sandstone body types. These sandstone bodies exhibit high amplitudes and can take on box, bell-shaped, toothed bell-shaped, and positively rhythmic forms. The vertical distribution of sandstone bodies primarily consists of two or three periods of vertical superposition (Figure 15a) or isolated vertical divisions (Figure 15b). The superimposed sandstone bodies have a favorable potential for the formation of large-scale effective reservoirs.

The porosity levels in tidal channels and sand flats are notably higher compared to mudflats, lime-mud flats, and mud flats. In the western region of the study area, the average porosity of single sandstone bodies in tidal channel deposits is approximately 5%, while sand flat deposits exhibit an average porosity ranging from 4.5% to 5%. Conversely, in the eastern region, the average porosity drops to around 4%, with negligible development of sand flat deposits. Ash flats and mud flats exhibit poor physical properties, making them unfavorable for reservoir formation (Figure 16a). The distribution of physical properties among different types of sandstone bodies aligns, indicating complex controlling factors for effective reservoirs. By considering variations in sandstone body stacking modes and comparing the physical properties of individual sandstone bodies, it is observed that the average porosity of Type A sandstone bodies within each area of the study ranges from 4% to 6%, which is significantly higher than that of Type B sandstone bodies by 3% to 4% (Figure 16b). Consequently, when identifying high-quality reservoirs, the comprehensive assessment of sedimentary facies and sandstone body types allows for the differentiation of reservoirs based on their physical characteristics. Type A sandstone bodies are predominantly found in tidal channels, the primary sections of tidal channels, and the central portions of sand flats. They exhibit thicknesses ranging from 0.3 m to 11.2 m, with an average thickness of 3.6 m. Moreover, over 75% of the single sandstone bodies possess a thickness exceeding 1 m. Furthermore, these areas of sandstone body distribution constitute regions with high-quality reservoirs.

Through the analysis of the correlation between various types of sandstone bodies and high-quality reservoirs, it has been observed that composite superimposed sandstone bodies facilitate the creation of efficient reservoirs. This can be attributed to several factors. Firstly, such reservoirs possess favorable original pore structures characterized by coarser clastic particles, well-sorted sediments, limited gravel content, and thick individual sand layers without many interlayers. These features increase the probability of fluid seepage during diagenesis, thereby establishing a spatial foundation for subsequent diagenetic transformations, especially dissolution processes.

5.2. Control of diagenesis on reservoir quality

Sedimentary facies have a significant influence on the characteristics of the sandstone body and its original pore structure, thereby controlling the occurrence of diagenesis within the sandstone body and influencing the evolution of reservoir physical properties (Zhang et al., 2016). Diagenesis takes place within a fluid-rock coexisting diagenetic system, where the dynamic balance of pressure, temperature, and fluid properties plays a crucial role. Consequently, diagenesis results in either the destruction or construction of the reservoir, ultimately affecting its compaction or development. (Sallam et al., 2019; Zhang et al., 2022).

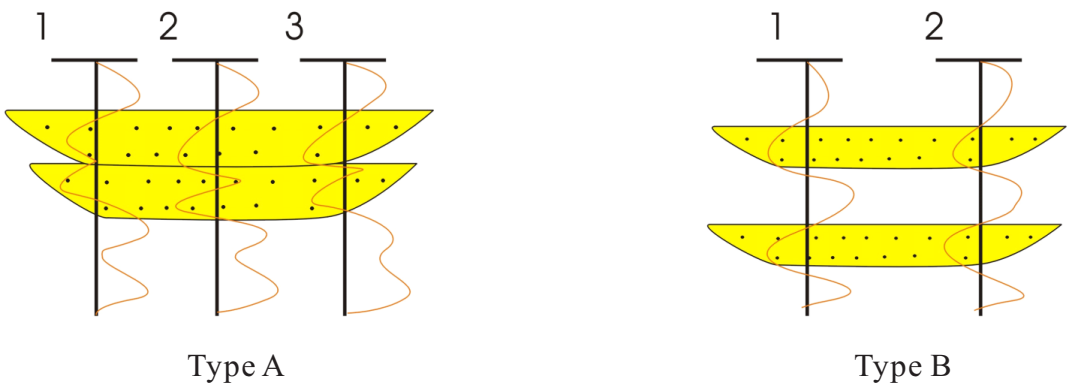

Figure 15. Two typical sand body structures in the study area, a. 2 to 3 stage sandstone body vertical superposition development, b. isolated development of sand bodies in vertical direction.

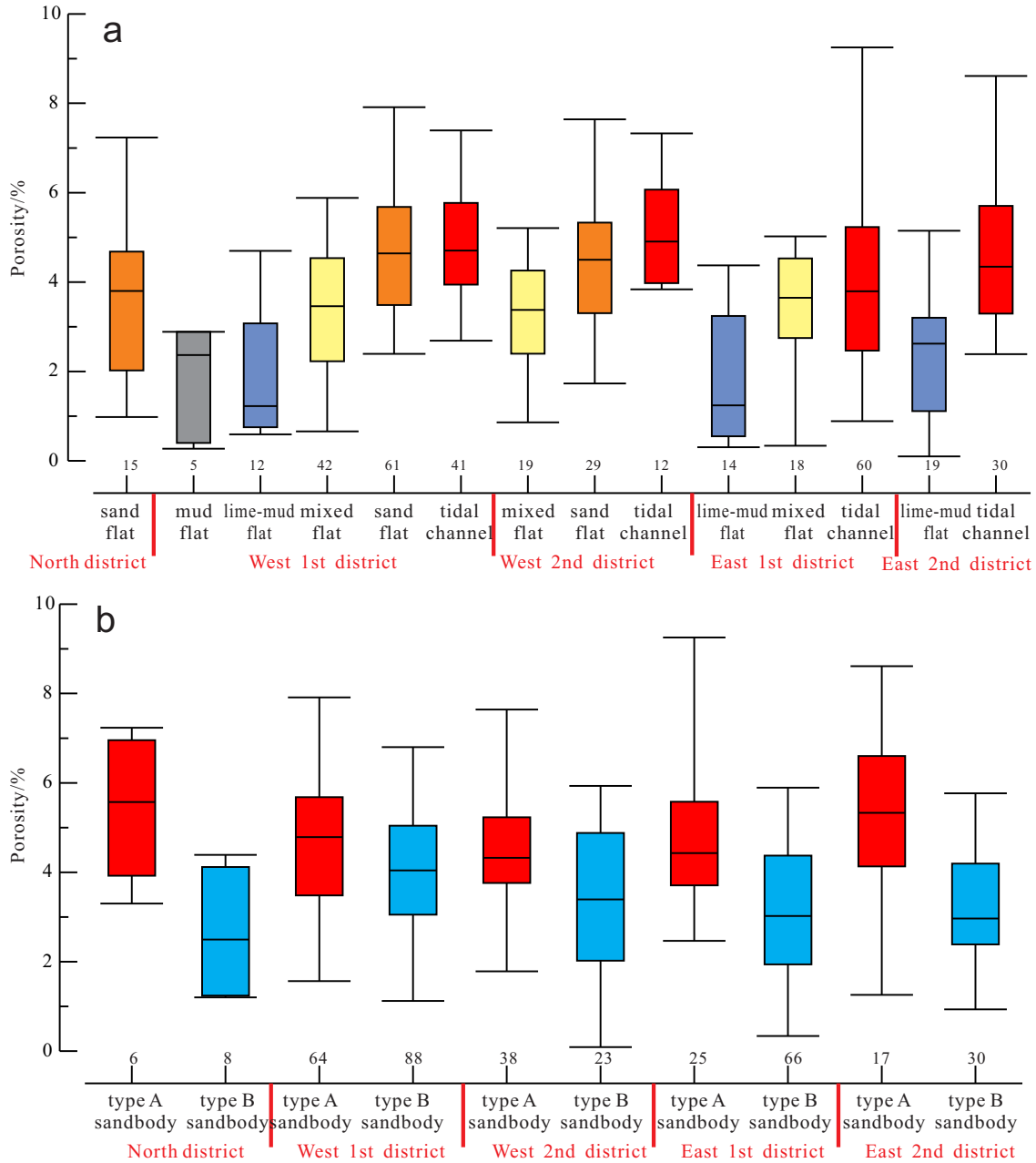

Figure 16. Comparison of physical properties of sandstones of different sedimentary facies (a) and sandstone body types (b) in various regions of Gaoqiao area.

Compaction and cementation play significant roles in the pore destruction of the Benxi Formation (Li et al., 2021). Quantitative analysis reveals that the Benxi Formation has experienced substantial compaction, ranging from medium to strong levels of cementation. This compaction has led to an absolute porosity loss ranging from 23.5% to 36.5%, with an average of 31.55%. On the other hand, cementation has caused an absolute porosity loss ranging from 1% to 13%, with an average of 4.15%. Consequently, compaction emerges as the primary driving factor behind the densification of the Benxi Formation sandstone, with subsequent cementation intensifying the extent of damage (Figure 17).

Intense compaction predominantly occurs in the upper portion of thin or thick normal graded sandstone bodies characterized by a rich matrix and plastic lithic

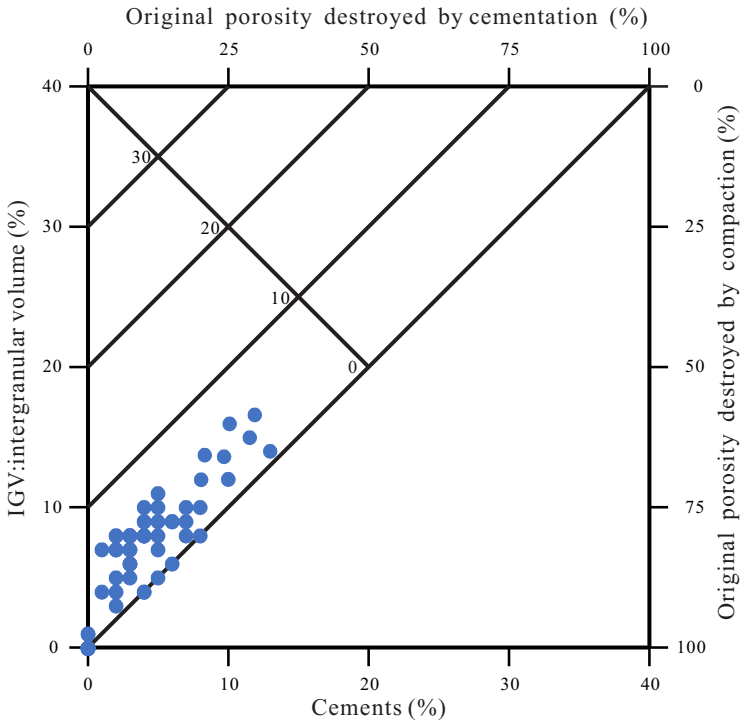

Figure 17. Cross plot of the effect of mechanical compaction and cementation on porosity reduction according to the corrected diagram proposed by Houseknecht (1987).

fine sandstones. Additionally, it frequently develops at the boundary where thin and thick sandstone bodies interface with mudstone. These regions exhibit weak compaction resistance due to the low proportion of rigid particles and the fine particle size of the debris present in the sandstone. The result of strong compaction in these regions is the total obliteration of the original pore structure within these sandstones (Figure 18a).

The robust cementation observed within the Benxi Formation is primarily characterized by the presence of authigenic quartz and calcite cementation. This is evident in the calcified zone or calcified edge of calcite within the sandstone near the mudstone-sandstone junction, as well as the pronounced siliceous cementation zone found internally within the medium-thick sandstone bodies (Figure 18a).

Throughout the early compaction phase, the mudstone exhibits weak resistance to compaction, resulting in a continuous increase in pore fluid pressure. To maintain equilibrium within the system, pore fluid migrates from the high-pressure zone of the mudstone towards the sandstone. This fluid migration occurs under the catalytic influence of various acidic waters. During this process, numerous Ca^{2+} ions are released from various sources, including syngenetic, supergene, and deeply buried diagenetic rocks. Consequently, there is an enrichment of Ca^{2+} ions within the original pore fluid. The contact between the sandstone and the mudstone provides ample space for compaction and facilitates cementation. This contact also serves as a source of cement supply for calcite cementation (Houseknecht, 1987; Liu et al., 2019; Zhang et al., 2022).

Intense enlargement of quartz commonly leads to reservoir compaction following early dissolution in sandstone bodies. The oversaturation of pore fluid SiO_2, irrespective of the sealing characteristics of the diagenetic system, triggers the precipitation of SiO_2 as solid cement in the form of quartz overgrowth or authigenic quartz, causing damage to the pore space (Robinson and Gluyas, 1992; Xi et al., 2015). During the early diagenetic stage, the edges of mineral grains within the sandstone body are relatively unaffected by clay minerals and other cements, resulting in the predominant production of quartz. This quartz production contributes to the closure of the sandstone diagenetic system. The extensive dissolution typically gives rise to pronounced cementation with intergranular authigenic quartz. As burial depth increases, compaction continues to alter the pore structure of the sandstone, resulting in a decrease in porosity. Subsequently, various clay minerals form different types of cementation on the

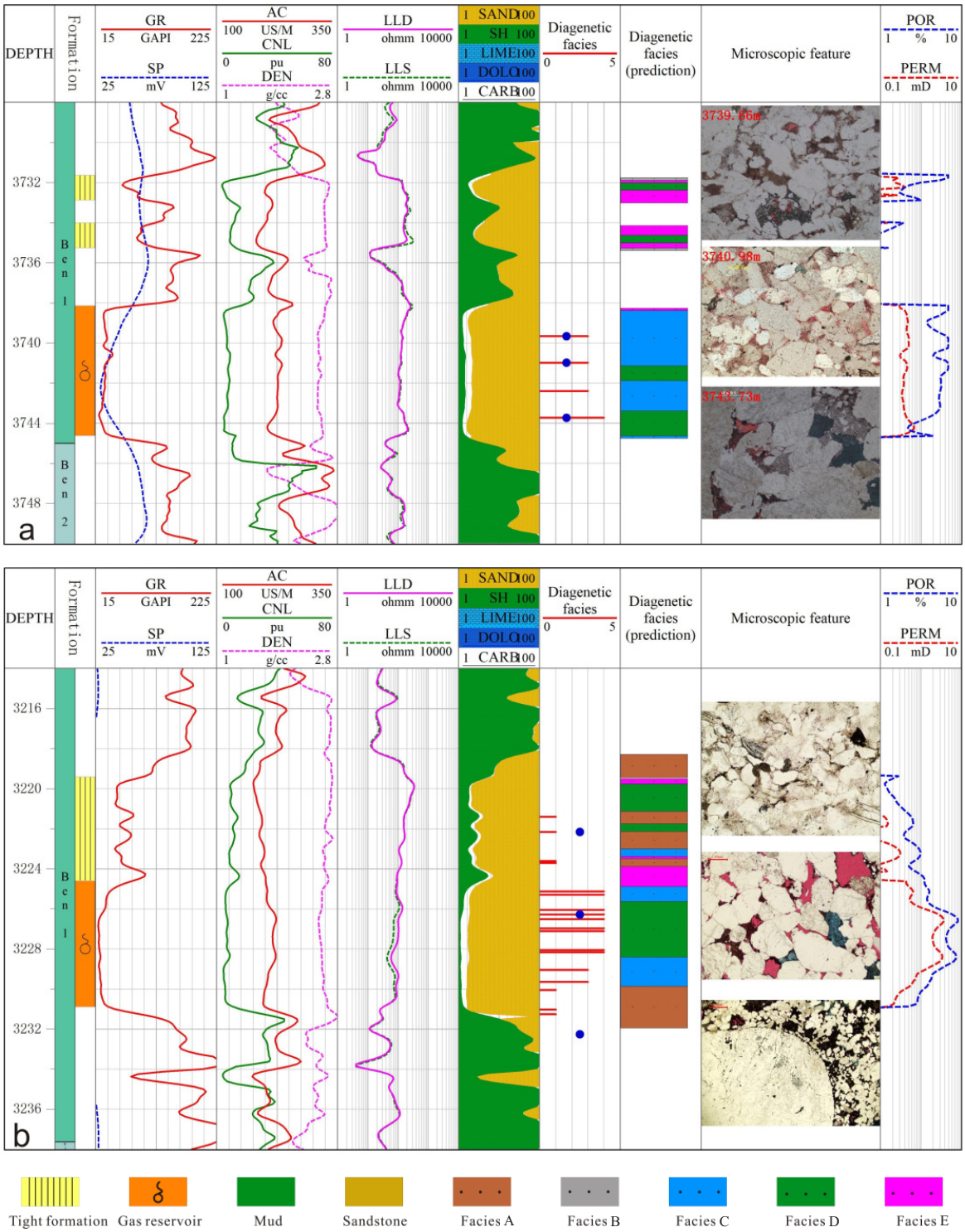

Figure 18. Comprehensive Profile of Single Well Reservoir and Diagenesis Characteristics. a. well S427; b. well S469.

surfaces of mineral particles. While dissolution and clay mineral transformation contribute a significant amount of SiO_2 for siliceous cementation, the primary manifestation of siliceous cementation is typically observed as authigenic microcrystalline quartz within intergranular pores. This quartz displays a higher degree of idiomorphism due to the loss of growth boundaries associated with quartz enlargement (Houseknecht, 1987; Robinson and Gluyas, 1992).

The sandstone bodies within the Benxi Formation exhibit distinct diagenetic variations, resulting in pronounced heterogeneity in pore structure and physical properties (Bjørlykke, 2014; Wang et al., 2017). In the same sandstone body, the boundary sections are characterized by significant compaction and strong cementation, while the middle portions tend to form high-quality reservoirs (Figure 18b). The presence of numerous well-developed pores within these medium-thick sandstone reservoirs can be attributed to several key factors. During the compaction process, water from the adjacent mudstone continuously drains into the sandstone with developed pores, aided by the effective sealing provided by the thick mudstone. This sealing system retains the sandstone pore fluid effectively, with the pore fluid supporting part of the overlying formation's load. As a result, it reduces vertical effective stress and inhibits mechanical compaction, thus preserving primary intergranular pores. Furthermore, in the later stages of hydrocarbon generation, the acid discharge resulting from organic matter promotes dissolution in the vicinity of the primary pore development zone within the sandstone body, facilitated by spatial development (Figure 18b). This spatial development enhances fluid flow, providing conducive conditions for dissolution processes. Consequently, the sandstone bodies of the Benxi Formation exhibit notable diagenetic variations, leading to heterogeneity in their pore structure and physical properties.

5.3. Diagenesis difference in different sedimentary facies zones

Given the comprehensive consideration of sedimentation's influence on sandstone body structure and diagenesis, as well as previous studies on the sequence evolution model of the Benxi Formation in the area, this study aims to compare the microscopic diagenetic characteristics within different sedimentary facies belts. Building upon the findings of Liu et al. (2021), it has been proposed that the study area exhibits mixed sedimentary strata consisting of terrigenous clastic rocks and carbonate rocks within the Benxi Formation. Consequently, this investigation elucidates the distribution characteristics of clastic tidal flat, mixed tidal flat, and mixed lagoon sediments in an east-west direction, while also recognizing their distribution characteristics on a two-dimensional plane.

The Benxi Formation primarily accumulates on the weathering crust of the Lower Paleozoic peneplain, filling its topography. Vertically, the Benxi Formation can be divided into two third-order sequences, namely the Ben 2 and the Ben 1 members. Each sequence exhibits a distinct structure consisting primarily of the Transgressive Systems Tract (TST) and the High Stand Systems Tract (HST). (Xi et al., 2015; Liu et al., 2021).

In the transgressive system tract (TST), a layer of Ferrolite mudrock is prominent, while interbedded sandstone and mudstone formations are observed in the upper section. In the highstand system tract (HST), sandstone and mudstone deposits are present. The overall sedimentary pattern is indicative of a gradual transgression with localized regression. Peperite formations are notably absent in this specific section. Thin sand flat sandstone bodies are developed within the clastic tidal flat area, while tidal channel sandstone bodies are prominent in the mixed tidal flat area.

Limestone formations are prominently developed at the base of the Ben 1 Member. The lithological assemblages within the TST, influenced by the sedimentary area, exhibit a variety of sequences from bottom to top. Within the clastic tidal flat sedimentary area, the lithology comprises medium-coarse sandstone, followed by sand-mudstone and mudstone layers. In the mixed tidal flat area, fine sandstone, siltstone, mudstone, and limestone are observed. The transitional zone between the mixed lagoon and mixed tidal flat reveals the presence of limestone, fine sandstone, silt, and mudstone. The mixed lagoon itself is characterized by multiple interbedded limestone and mudstone layers. The distribution of mudstone and coal seams within the HST remains relatively stable (Figure 19). In contrast, the TST displays a greater thickness compared to the HST, indicative of a multistage continuous transgression. Sand flat sandstone bodies are preferentially developed within the clastic tidal flat area, while thick tidal channel sandstone bodies are prominent in the mixed tidal flat area.

In conjunction with the subdivision of diagenetic facies, a comparison of the microscopic diagenetic characteristics of sandstone in various sedimentary facies belts within the region is presented below:

1. Facies A and B are found in thin sand flat and sand-mud flat sandstone bodies within the clastic rock tidal flat area of the Ben 1 Member. These facies exhibit pronounced compaction and siliceous cementation, resulting in minimal pore development (Figure 19a).

2. Facies B is observed at the upper and lower boundaries of the mixed tidal flat and tidal channel sandstone bodies in the Ben 1 Member. These facies experience moderate to strong compaction, chlorite rim cementation, strong siliceous cementation, and limited pore development (Figure 19b).

3. Facies C occurs in the central part of the sand flat and tidal channel sandstone bodies within the middle section of the mixed tidal flat in the Ben 2 Member. These facies undergo substantial compaction, moderate siliceous cementation, medium to strong dissolution processes, and the development of secondary dissolution pores (Figure 19c).

4. Facies D is present in the middle portion of the mixed tidal flat and tidal channel sandstone bodies within the Ben 1 and Ben 2 members. These facies exhibit moderate compaction, chlorite rim cementation, and a high degree of primary pore development (Figure 19d).

5. Facies E is observed at both the upper and lower boundaries of the tidal channel sandstone bodies in the transitional zone between the mixed tidal flat and mixed lagoon areas. These facies undergo moderate compaction, strong cementation, with dolomite cementation leading to near-complete porosity loss (Figure 19e).

Overall, the sand flat of the clastic tidal flat in the Ben 2 Member and the tidal channel sandstone bodies within the mixed tidal flat in the Ben 1 and Ben 2 members are favorable locations for the development of high-quality reservoirs. This is attributed to the significant development of sandstone facies C and D, as well as the presence of well-developed pores.

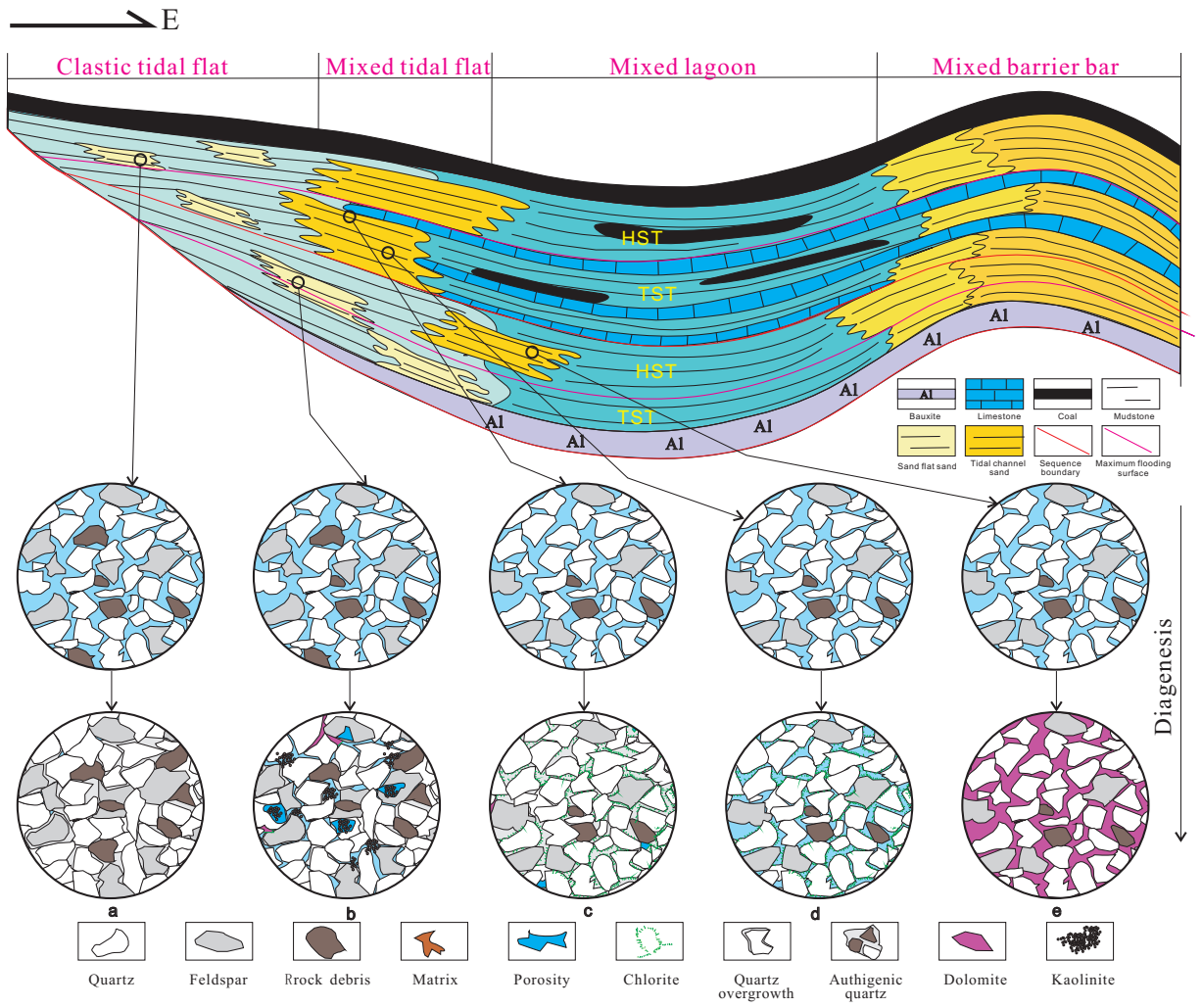

Figure 19. Diagenesis characteristics of sandstone bodies under different sedimentary modes of the Benxi Formation in the Gaoqiao area (sedimentary model modified after Liu et al., 2018).

6. Conclusion

1. The paleogeomorphology of the study area before the deposition of the Benxi Formation exhibits a general landform combination of highland-slope-groove-lake basin, with higher elevations in the west and lower elevations in the east. The northern region features steep slopes, whereas the southern region is characterized by gentle slopes. The Benxi Formation overlies the area from east to west, with paleocurrents predominantly flowing from the west, southwest to the east and northeast, following the distribution pattern of fluid potential.

2. The study area is situated in the eastern part of the north-south central paleo-uplift and was originally an area occupied by the North China Sea during its early stages. As a result of tidal action, tidal flat deposits were formed. The Benxi Formation primarily consists of terrigenous clastic rocks, interspersed with mixed strata composed of both terrigenous clastic rocks and carbonate rocks. The progression from west to east reveals the presence of clastic tidal flat deposits, followed by mixed tidal flat deposits, and finally mixed lagoon deposits that are predominantly developed in the northeastern part of the study region.

3. Sedimentary facies serve as the geological foundation that influences reservoir properties. The sedimentary environment determines the original composition and structure of the reservoir rocks, and subsequently controls diagenetic processes. Sandstone bodies formed through the superimposition of tidal channels and sand flats have a favorable potential for the development of extensive and effective sandstone reservoirs. The processes of compaction and cementation contribute to the densification of the Benxi Formation sandstone. The dissolution and preservation of primary pores play a crucial role in the development of high-quality reservoirs.

4. Through the analysis of the sandstone characteristics within varioussedimentary facies belts in the sequence evolution model of the Benxi Formation, it becomes evident that the sand flats of the clastic tidal flat in the Ben 2 Member and the tidal channel sandstone bodies of the mixed tidal flat in the Ben 1 and Ben 2 members showcase a high degree of internal pore development. This favorable attribute enhances the potential for the development of high-quality reservoirs.

Funding

This study was financially supported by the General Project of Chongqing Natural Science Foundation (No. CSTB2022NSCQ-MXS1642, cstc2021jcyj-msxmX08907 and Joint Fund for Innovation and Development of Chongqing Natural Science Foundation (No: 2023NSCQ-LZX0184).

Acknowledgment

We would like to thank the PetroChina Changqing Oilfield Company for providing samples and data. We thank all editors and anonymous reviewers for their helpful comments and suggestions.

Conflicts of interest

The authors declare that they have no conflicts of interest.

References

Anees A, Zhang HC, Ashraf U, Wang R, Thanh HV et al. (2022). Sand-ratio distribution in an unconventional tight sandstone reservoir of Hangjinqi area, Ordos Basin: Acoustic impedance inversion-based reservoir quality prediction. Frontiers in Earth Science 10: 1018105. https://doi.org/10.3389/feart.2022.1018105

Bezzi A, Casagrande G, Martinucci D, Pillon S, Del Grande C et al. (2019). Modern sedimentary facies in a progradational barrier-spit system: Goro lagoon, Po delta, Italy. Estuarine Coastal and Shelf Science 227: 106323. https://doi.org/ 10.1016/j.ecss.2019.106323

Bjørlykke K (2014). Relationships between depositional environments, burial history and rock properties. Some principal aspects of diagenetic process in sedimentary basins. Sedimentary Geology 301: 1–14. https://doi.org/10.1016/j.sedgeo. 2013.12.002

Crundwell FK (2014). The mechanism of dissolution of minerals in acidic and alkaline solutions: part II. Application of a new theory to silicates, aluminosilicates and quartz. Hydrometallurgy 149: 265–275. https://doi.org/10.1016/j.hydromet. 2014.07.003

Cui XY, Radwan AE (2022). Coupling relationship between current in-situ stress and natural fractures of continental tight sandstone oil reservoirs. Interpretation 10 (3): 9-21. https://doi.org/10.1190/INT-2021-0200.1

Dong SQ, Zeng LB, Lyu WY, Xia DL, Liu GP et al. (2020). Fracture identification and evaluation using conventional logs in tight sandstones: A case study in the Ordos Basin, China. Energy Geoscience 1 (3-4): 115–123. https://doi.org/10.1016/j.engeos.2020.06.003

Ehrenberg SN (1990). Relationship between diagenesis and reservoir quality in sandstones of the Garn formation, Haltenbanken, mid-norwegian continental shelf. AAPG Bulletin 74 (10): 1538–1558. https://doi.org/10.1306/0C9B2515-1710-11D7-8645000102C1865D

Folk RL (1980). Petrology of Sedimentary Rocks. Texas, Hemphill Publishing, Austin, pp. 182.

Fu JH, Wei XS, Nan JX, Shi XH (2013). Characteristics and origin of reservoirs of gas fields in the Upper Paleozoic tight sandstone, Ordos Basin. Journal of Palaeogeography 15 (4): 529–538 (in Chinese with English abstract). https://doi.org/10.605/gdlxb.2013.04.042

Fu JH, Deng XQ, Wang Q, Li JH, Qiu JL et al. (2017). Densification and hydrocarbon accumulation of triassic Yanchang Formation Chang 8 member, Ordos Basin, NW China: evidence from geochemistry and fluid inclusions. Petroleum Exploration and Development 44 (1): 48–57. https://doi.org/10.11698/PED.2017.01.06

Feng JP, Ouyang ZJ, Chen QH, Li WH (2021). Sedimentary characteristics of the upper Carboniferous in Ordos Basin and its adjacent areas. Journal of Palaeogeography (Chinese Edition) 23 (1): 53–64. https://doi.org/10.7605/gdlxb.2021.01.004

Guo SY, Zhang GQ, Chen SW (2009). Study on sedimentary facies of mixed clastic-carbonate sediments strata system in epicontinental sea A case of Daniudi Gasfield in northeastern Ordos. Journal of Palaeogeography 11 (6): 611–627 (in Chinese with English abstract). https://doi.org/10.7605/gdlxb.2009.06.002

Hodgkinson J, Cox ME, McLoughlin S, Huftile GJ (2008). Lithological heterogeneity in a back-barrier sand island: Implications for modelling hydrogeological frameworks. Sedimentary Geology 203(1-2):64–86. https://doi.org/10.1016/j.sedgeo.2007.11.001

Hou YD, Chen AQ, Zhao WB, Dong GD, Yang S et al. (2018). Analysis on the depositional environment of carboniferous Benxi Formation tidal-delta sandstone body complex, Ordos Basin, China. Journal of Chengdu University of Technology. Science & Technology Edition 45 (4): 393–401 (in Chinese with English abstract). https://doi.org/10.3969/j.issn.1671-9727.2018.04.01

Houseknecht DW (1987). Assessing the relative importance of compaction processes and cementation to reduction of porosity in sandstones. AAPG Bulletin 71 (6): 633–642. https://doi.org/10.1306/9488787F-1704-11D7-8645000102C1865D

Huang SJ, Huang KK, Feng WL, Tong HP, Liu LH et al. (2009). Mass exchanges among feldspar, kaolinite and illite and their influences on secondary porosity formation in clastic diagenesis — a case study on the upper paleozoic, Ordos basin and xujiahe formation, Western Sichuan depression. Geochimica 38 (5): 498–506 (in Chinese with English abstract). https://doi.org/ 10.19700/j.0379-1726.2009.05.009

Huang YT, Kane IA, Zhao Y (2020). Effects of sedimentary processes and diagenesis on reservoir quality of submarine lobes of the Huangliu Formation in the Yinggehai Basin, China. Marine and Petroleum Geology 120: 104526. https://doi.org/10.1016/j.marpetgeo.2020.104526

Jia LB, Zhong DK, Sun HT, Yan RT, Zhang CL et al. (2019). Sediment provenance analysis and tectonic implication of the Benxi Formation, Ordos Basin. Acta Sedimentol. Sinica 37 (5): 1087–1103 (in Chinese with English abstract). https://doi.org/10.14027/j.issn.1000-0550.2019.014

Jiu B, Huang WH, Li Y, He MQ (2021). Influence of clay minerals and cementation on pore throat of tight sandstone gas reservoir in the eastern Ordos Basin, China. Journal of Natural Gas Science and Engineering 87: 103762. https://doi.org/10.1016/j.jngse.2020.103762

Li YJ, Zhao Y, Yang RC, Fan AP, Li FP (2010). Detailed sedimentary facies of a sandstone reservoir in the eastern zone of the Sulige gas field, Ordos Basin. Mining Science and Technology (China) 20 (6): 891–897. https://doi.org/10.1016/S1674-5264(09)60302-1

Li Y, Zhang JW, Li J, He J, Sun GM et al. (2014). A study on sedimentary microfacies of Benxi Formation and its controlling effect on gas enrichment in Yanchang district of Ordos Basin. Northwestern Geology 47 (2): 216–222 (in Chinese with English abstract). https://doi.org/10.3969/j.issn.1009-6248.2014.02.027

Li YL, Yu XH, Shan X, Du YH, Zhou JS et al. (2016). Provenance and sedimentary facies of He8 member of Xiashihezi formation in southeastern Ordos basin. Journal of Northeast Petroleum University 40 (03): 51–60 (in Chinese with English abstract). https://doi.org/10.3969/j.issn.2095-4107.2016.03.007

Li Y, Wang ZS, Pan ZJ, Niu XL, Yu J et al. (2019). Pore structure and its fractal dimensions of transitional shale: A cross section from east margin of the Ordos Basin, China. Fuel 241: 417–431. https://doi.org/10.1016/j.fuel.2018.12.066

Li J, Zhang X, Tian JC, Liang QS, Cao TS (2021). Effects of deposition and diagenesis on sandstone reservoir quality: a case study of Permian sandstones formed in a braided river sedimentary system, northern Ordos Basin, Northern China. Journal of Asian Earth Science 213 (15): 104745.https://doi.org/10.1016/j.jseaes.2021.104745

Liang F, Huang WH, Niu J (2018). Provenance analysis of Permain Shan1 and He 8 Formation in Permian in Southwest Ordos Basin. Acta Sedimentologica Sinica 36 (01): 142–153 (in Chinese with English abstract) https://doi.org/10.3969/j.issn.1000-0550.2018.016

Liu M, Liu Z, Liu J, Zhu W, Huang Y et al. (2014). Coupling relationship between sandstone reservoir densification and hydrocarbon accumulation: a case from the Yanchang Formation of the Xifeng and Ansai areas, Ordos Basin. Petroleum Exploration and Development. 41 (2): 185–192. https://doi.org/10.11698/PED.2014.02.05

Liu MJ, Liu Z, Wang P, Pan GF (2016). Diagenesis of the Triassic Yanchang Formation tight sandstone reservoir in the Xifeng-Ansai area of Ordos Basin and its porosity evolution. Acta Geologica Sinica - English Edition 90 (3): 956–970. https://doi.org/10.3969/j.issn.1000-9515.2016.03.017

Liu GZ, Zhang DD, Li P (2018). Sedimentary characteristics of Upper Paleozoic mixed deposits in southeastern Ordos. Journal of Southwest Petroleum University:Science & Technology Edition 40 (2): 25–33 (in Chinese with English abstract). https://doi.org/10.11885pssfl.16745086.2016.1020,02

Liu M, Gluyas J, Wang W, Liu Z, Liu J et al. (2019). Tight oil sandstones in Upper Triassic Yanchang Formation, Ordos Basin, N. China: reservoir quality destruction in a closed diagenetic system. Geological Journal 54 (6): 3239–3256. https://doi.org/10.1002/gj.3319

Liu GZ, Gao W, Wei JS, Tang W (2021). Sedimentary characteristics and sequence stratigraphy in a mixed silicilasticcarbonate depositional system Case study of Benxi Formation in Gaoqiao area,Ordos Basin. Natural Gas Geoscience 32 (3): 382–392 (in Chinese with English abstract). https://doi.org/10.11764/j.issn.1672-1926.2020.11.002

Morad S, Al Ramadan K, Ketzer JM, De Ros LF (2010). The impact of diagenesis on the heterogeneity of sandstone reservoirs: a review of the role of depositional facies and sequence stratigraphy. AAPG Bulletin 94 (8): 1267–1309. https://doi.org/10.1306/04211009178

Ng C, Vega CS, Maranhão MDAS (2019). Mixed carbonate-siliciclastic microfacies from Permian deposits of Western Gondwana: Evidence of gradual marine to continental transition or episodes of marine transgression. Sedimentary Geology. 390: 62–82. https://doi.org/10.1016/j.sedgeo.2019.07.006

Okunuwadje SE, Bowden SA, Macdonald DIM (2020). Diagenesis and reservoir quality in high-resolution sandstone sequences: An example from the Middle Jurassic Ravenscar sandstones, Yorkshire Coast UK. Marine and Petroleum Geology 118: 104426. https://doi.org/10.1016/j.marpetgeo.2020.104426

Qiao JC, Zeng JH, Jiang S, Ma Y, Feng S et al. (2020). Role of pore structure in the percolation and storage capacities of deeply buried sandstone reservoirs: A case study of the Junggar Basin, China. Marine and Petroleum Geology 113: 104–129. https://doi.org/10.1016/j.marpetgeo.2019.104129

Radwan AE (2021). Modeling the depositional environment of the sandstone reservoir in the middle Miocene Sidri Member, Badri field, Gulf of Suez basin, Egypt: integration of gamma-ray log patterns and petrographic characteristics of lithology. Natural Resources Research 30 (1): 431-449. https://doi.org/10.1007/s11053-020-09757-6

Radwan AE (2022). Provenance, depositional facies, and diagenesis controls on reservoir characteristics of the middle Miocene Tidal sandstones, Gulf of Suez rift basin: integration of petrographic analysis and gamma-ray log patterns. Environmental Earth Sciences 81 (15): 1-15. https://doi.org/10.1007/s12665-022-10502-w

Ran YX, Zhou X (2020). Geochemical characteristics and genesis of tight gas in Shahezi Formation, Xujiaweizi Fault Depression, North Songliao Basin, China. Journal of Natural Gas Geoscience 5 (2): 69–79. https://doi.org/10.1016/j.jnggs.2020.02.003

Robinson AG, Gluyas JG (1992). Duration of quartz cementation in sandstones, North Sea and Haltenbanken basins. Marine and Petroleum Geology 9: 324–327. https://doi.org/10.1016/0264-8172(92)90081-O

Shen YL, Guo YH, Li ZF, Wei XS, Jia ZG (2009). Sequence stratigraphy of Benxi-Taiyuan Formation in eastern Ordos Basin. Acta Geoscientica Sinica 30 (2): 187–193 (in Chinese with English abstract).

Sallam ES, Afife MM, Fares M, Van Loon AJ, Ruban DA (2019). Sedimentary facies and diagenesis of the lower miocene rudeis formation (southwestern offshore margin of the Gulf of Suez, Egypt) and implications for its reservoir quality. Marine and Petroleum Geology 413: 48–70. https://doi.org/10.1016/j.margeo.2019.04.004

Wei YP, Wang Y (2004). Comparison of enrichment patterns of various energy resources in Ordos Basin. Oil Gas Geology 25 (4): 385–392 (in Chinese with English abstract).

Wang XZ (2014). Major breakthrough of gas exploration in Yanchang blocks and its significance. Oil Gas Geology 35 (1): 1–9 (in Chinese with English abstract). https://doi.org/10.11743/ogg20140101

Wang M, Tang HM, Zhao F, Liu S, Yang Y et al. (2017). Controlling factor analysis and prediction of tight sandstone reservoir quality: A case study of He8 Member in eastern Sulige Gas field, Ordos Basin, China. Journal of Natural Gas Science & Engineering 46: 680-698. https://doi.org/10.1016/j.jngse.2017.08.033

Wang M, Tang HM, Tang HX, Liu S, Zhang LH et al. (2019a). Impact of Differential Densification on the Pore Structure of Tight Gas Sandstone: Evidence from the Permian Shihezi and Shanxi Formations, Eastern Sulige Gas Field, Ordos Basin, China. Geofluids 2019: 1-25. https://doi.org/10.1155/2019/4754601

Wang M, Tang HM, Zeng M, Lin G, Cheng YL et al. (2019b). Diagenesis and diagenetic facies distribution prediction of the Chang 8 tight oil reservoir in Maling area, Ordos Basin, NW China.Turkish journal of Earth Sciences 28 (3): 457-469. https://doi.org/10.3906/yer-1809-13

Wang HQ, Chen M, Wei SM, Lu YH, Nie Z et al. (2020). The influence of barrier coastal sedimentary system lost circulation in sandstone. Journal of Petroleum Science & Engineering. 185: 106654. https://doi.org/10.1016/j.petrol.2019.106654

Wang SL, Yang XR, Lu YY, Su PD, Liu D et al. (2022). Densification mechanism of deep low-permeability sandstone reservoir in deltaic depositional setting and its implications for resource development: A case study of the Paleogene reservoirs in Gaoshangpu area of Nanpu sag, China. Frontiers in Earth Science, 10: 996167. https://doi.org/10.3389/feart.2022.996167

Xi KL, Cao YC, Jaren J, Zhu RK, Bjørlykke K et al. (2015). Diagenesis and reservoir quality of the lower cretaceous quantou Formation tight sandstones in the southern songliao basin. China. Sedimentary Geology 330: 90–107. https://doi.org/10.1016/j.sedgeo.2015.10.007

Yan HJ, He DB, Xu WZ, Wang GT, Ji G et al. (2016). Paleotopography restoration method and its controlling effect on fluid distribution:a case study of the gas reservoir evaluation stage in Gaoqiao,Ordos Basin.Acta Petrolei Sinica.37 (12): 1483–1494 (in Chinese with English abstract). https://doi.org/10.7623/syxb201612004

Zhao JX, Chen HD, Xiang F (2003). The possibility of rebuilding paleogeomorphology before basin deposition by high-resolution sequence stratigraphy. Journal of Chengdu University of Technology, Science& Technology Edition 30 (1): 76–81 (in Chinese with English abstract).

Zhang HB, Peng J, Yang SJ, Lu M, Xia QS et al. (2016). Diagenesis and controlling factors of tight sandstone reservoirs: a case study of the lower member of Silurian Kepingtage Formation in Shuntuoguole area, Tarim Basin. Petroleum Geology & Experiment 38 (04): 543–550 (in Chinese with English abstract). https://doi.org/10.11781/sysydz201604543

Zhang DF, Li CS, Liu WX, Ma GW, Li WH et al. (2021). Sedimentary characteristics of the upper Permian in Ordos Basin and its adjacent areas. Journal of Palaeogeography. Chinese Edition) 23 (1): 93–104 (in Chinese with English abstract). https://doi.org/10.7605/gdlxb.2021.01.007

Zhang Q, Wu XS, Radwan AE, Wang BH, Wang K et al. (2022). Diagenesis of continental tight sandstone and its control on reservoir quality: A case study of the Quan 3 member of the cretaceous Quantou Formation, Fuxin uplift, Songliao Basin. Marine and Petroleum Geology 145: 105883. https://doi.org/10.1016/j.marpetgeo.2022.105883

Zheng DY, Pang XQ, Jiang FJ, Liu TS, Shao XH et al. (2020). Characteristics and controlling factors of tight sandstone gas reservoirs in the Upper Paleozoic strata of Linxing area in the Ordos Basin. Journal of Natural Gas Science & Engineering 93 (3): 637–659. https://doi.org/10.1016/j.jngse.2019.103135